5-9-1996

Fluorinated Polymer Films - Synthesis and Characterization

Anja Ulrike Schnurer
Portland State University

THESIS APPROVAL

The abstract and thesis of Anja Ulrike Schnurer for the Master of Science degree in Chemistry was presented May 9, 1996 and accepted by the thesis committee and the department.

COMMITTEE APPROVALS: [redacted]

Gary L. Gard

[redacted]

Dennis Barnum

[redacted]

Carl C. Wamser

[redacted]

Pavel Smejtek
Representative of the Office of Graduate Studies

DEPARTMENT APPROVAL [redacted]

David Peyton, Chair
Department of Chemistry

****

ACCEPTED FOR PORTLAND STATE UNIVERSITY BY THE LIBRARY

by [redacted] on 24 June 1996

Abstract

An abstract of the thesis of Anja Ulrike Schnurer for the Master of Science in Chemistry presented on May 9, 1996

Title: Fluorinated polymer films - synthesis and characterization

Three polyfluoroalkyl epoxides, (I $\overline{OCH_2CH}CH_2OCF_2CF_2SO_2F$, II $\overline{OCH_2CH}CH_2(CF_2)_8F$ and III $\overline{OCH_2CH}CH_2O(CF_2)CF(CF_3)SO_2F$) were photo-polymerized with a cycloaliphatic diepoxide (Cyracure UVR-6110) to form highly cross-linked glassy films.

Depth-dependent surface analysis with XPS show that these films are highly enriched with sulfonyl fluoride groups in the outer molecular surface. Film compositions of 17 % wt and more of the fluorinated I and III show surface characteristics of a film composed of 100 % wt of the polymerized sulfonyl fluoride epoxide monomer (at depths for 50 Å for each sample). Even films that are prepared with only 1 % wt or less (compound III) of the fluorinated epoxide result in a thick overlayer of sulfonyl fluoride. The results of FTIR (attenuated total reflectance) spectra support these conclusions. Secondary ion mass spectra show peaks that can be assigned to perfluoro and sulfonyl fluoride groups, thus

suggesting the formation of an overlayer of fluoroepoxide (within the sampling depth of this method, outer 15 Å). The above process holds great promise for forming fluorinated overlayers in mixtures where the total fluorine content is low. Extreme surface enrichment by the fluorinated epoxides like this is useful for applications where expensive or exotic fluorinated epoxides are necessary to form a strong overlayer, but comprising only small component additives of the total bulk mixture.

FLUORINATED POLYMER FILMS - SYNTHESIS AND CHARACTERIZATION

by

ANJA ULRIKE SCHNURER

A thesis submitted in partial fulfillment of the requirements for the degree of

MASTER OF SCIENCE

in

CHEMISTRY

Portland State University

1996

DEDICATION

dedicated to my parents

ACKNOWLEDGMENTS

I want to thank Dr. Gary Gard for his knowledge, for sharing it with me, for his never-ending patience and his will to help me anytime. If it wouldn't be for his support, this thesis would have never been written.

Rob Holcomb was a wonderful, patient help in the laboratory work involved, and a source of great information. Thank you for your help.

Dr. Robin Tergeson always knew things that others didn't, and also where to find rare, but necessary parts for the experiment.

Paul Nixon was the expert for the vacuum line, and of great help dealing with it. He taught me how to use it and was a great help.

Thanks to Dr. Grainger for doing the FTIR analysis of my samples.

Thanks to Dr. Castner for doing the XPS and contact angle analysis in his laboratory.

And I also want to thank Julia Renn for her mental support when things were rough. She is a real friend and I very much appreciated her help.

TABLE OF CONTENTS

LIST OF TABLES

LIST OF FIGURES

INTRODUCTION - REVIEW OF EPOXIDES

Fluorinated epoxides are an unique species of epoxides that are being used in a variety of polymer applications.

Various papers published in recent years report the use of fluorinated epoxides as antifoaming agents [1], adhesives for fluoroplastic adherents without surface treatment [2], fiber coating applications [3] [4], optical part bonding [5], bonding for fluoroplastics [6], solder resists [7], medical applications [8], moisture vapor barrier coating [9], protection of optical fibers against stress corrosion [10], marine coatings [11], and the use of fluoroepoxy for coating systems[12].

Table 1 shows a list of some of the known highly fluorinated epoxides [33]. The epoxy-group is defined as a chemical group consisting of an oxygen bond with two carbon atoms already united in some other way [13]. The simplest epoxy has to be a three membered ring called α -epoxy or 1,2 epoxy. Ethylene oxide ($\overline{OCH_2CH_2}$) is an example of this type, its name being oxirane. A very important property of epoxides is their ability to readily transform from the liquid to the solid state via polymerization. There are usually no by-products from this conversion. For example, the conversion can be accomplished by adding a curing agent (a chemically active agent). This agent either functions as a catalyst or takes part in the reaction and becomes bound into the chain. Depending on the type of reaction, heat may have to be applied.

Table 1 [33]

Highly Fluorinated Epoxides

Compound	bp, °C	Infrared, μ	
	—	—	
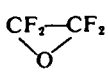	−63.5	6.2	
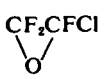	−22.0	6.5	
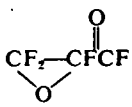	16	6.61	
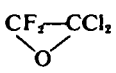	20.2	6.7	
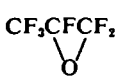	−27.4	6.43	
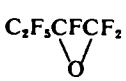	—	6.48	
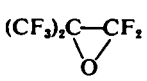	3	6.66	
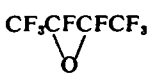	—	6.65	
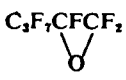	—	—	
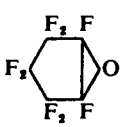	26.5	6.55	
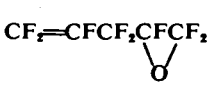	37	6.45 5.65 ($CF_2=CF$)	
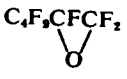		80–88	—
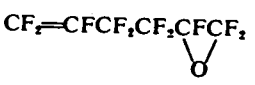		59	—
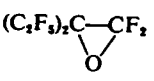		—	—
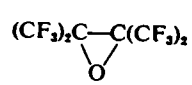		53–54	—

Compound	bp, °C	Infrared, μ
	53–55	6.7
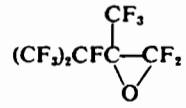	—	—
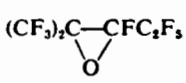	57	6.85
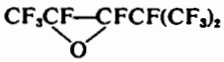	53	6.61
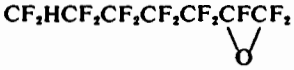	—	—
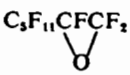	—	—
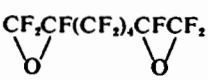	104	6.45
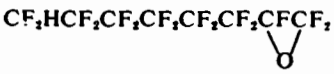	123	6.47
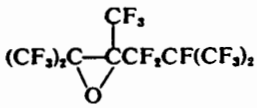	36–39/1 *mm*	7.2
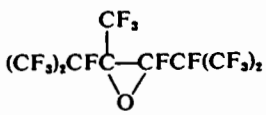	—	6.95
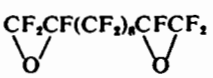	88/40 mm	—

The reactivity of the epoxy-ring differs, depending on its position in the chain - it can be terminal, internal or ring-situated. The cured structure can then be either a homopolymer or a heteropolymer.

Reactions of the epoxide group

The mechanism by which the epoxide group reacts is

1. Anionic[13]:

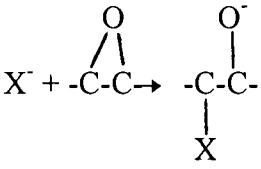

the ring opens to yield an anion. This anion is then activated and capable of reacting further (1).

2. Cationic[13]:

In the cationic reaction, the epoxy-group is opened by an active hydrogen, this leading to a new bond and a hydroxyl-group.

There are several ways for this mechanism to take place:

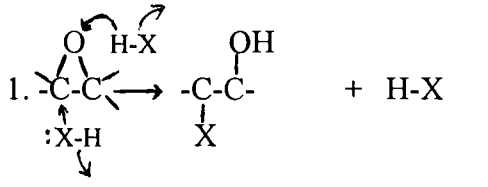

(2)

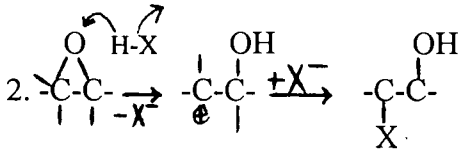

(3)

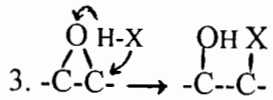

(4)

The basic curing agents used for epoxy-reactions are Lewis bases, inorganic bases, primary and secondary amines, and amides. Lewis bases are compounds that contain an atom with an unshared electron pair in its outer orbital [13]. They are attracted to areas in the molecules of reduced electron density. Lewis acids are compounds containing empty orbital positions in the outer shell of one of the atoms. They are attracted to areas of increased electron density.

Chain Propagation

The type of polymerization believed to take place in this work is called photoinitiated cationic polymerization, and is initiated by onium salts. Ethylene oxide and other epoxy derivatives do not polymerize by a radical mechanism, instead they polymerize readily by a cationic mechanism [15]. The propagation of the chain of these systems is based on the attack of a carbocation on the negatively polarized oxygen of the oxirane [16]. The initiation of the chain takes place either by another cation or by a strong electrophile, for example a Lewis acid or a protonic Bronsted acid.

Chain initiation:

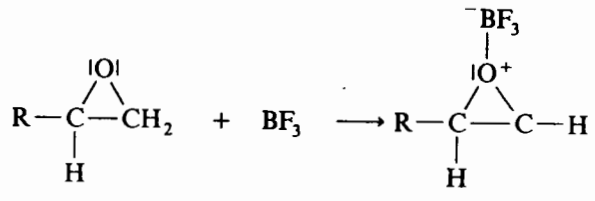

Oxirane **Boron trifluoride** (5)

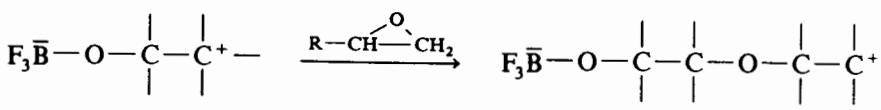

Carbocation (6)

The chain propagation is a fast reaction - this step is increased by the coulombic interaction between the carbocation and the negatively polarized ether oxygen. However, the data in table 2 illustrates that the strain in the three-membered ring is the most important structural part of the molecule that helps the reaction to proceed.

Table 2. Heat of Polymerization for cyclic ethers calculated from ring strain [17]

Monomer	Ring Size	dH (kcal/mol)
Ethylene oxide	3	22.6
Trimethylene oxide	4	19.3
Tetrahydrofurane	5	3.5
Dimethylene formal	5	6.2
Tetrahydropyran	6	-1.3
Trimethylene formal	6	0
Tetramethylene formal	7	4.7

The chain is terminated by a carbocation reacting with an adventitious nucleophile, a base for example, or uncommonly with the anion of the initiator. To avoid termination, the counter anion must have a very low nucleophilicity. Strong nucleophiles or bases would terminate the reaction immediately. A great advantage in this process is that water in small concentrations can be tolerated, and also oxygen (acts as a biradical) doesn't affect the cationic polymerization. The mechanical properties of epoxy polymers are very good: they are heat resistant, dimensionally stable, colorless, nontoxic, and chemically inert.

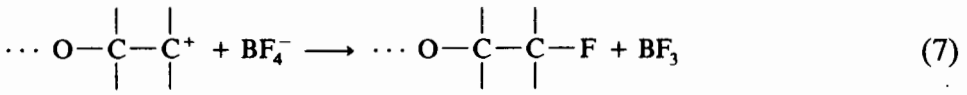

(7)

Polymerization of cyclic organic compounds [27]

An overall process of the ring-opening polymerization of cyclic compounds is shown in reaction eight:

$$\begin{array}{l} \text{A-B} \\ \quad | \quad | \\ \text{(A-B)}_n \end{array} \longrightarrow \text{(-A-B-)}_{n+1} \qquad (8)$$

In contrast to condensation reactions, polymerization does not result in the loss of a small molecule. The ring-opening polymerization does not involve a loss of multiple bonding enthalpy, instead, the driving force for olefin polymerization is the loss of unsaturation. Some of the cyclic organic compounds that have been polymerized include cyclic ethers, lactones (cyclic esters), lactams (cyclic amides) and imines (cyclic amines).

In the case of the epoxide polymerization the ring opening is due to a release of ring strain, as mentioned above. Ethylene oxide is a great example - it easily polymerizes to polyethylene oxide with either anionic or cationic catalysts. As mentioned earlier in this chapter, the cationic polymerization is initiated by Lewis acids and protonic reagents.

$$n \; \begin{array}{c} \text{O} \\ / \quad \backslash \\ \text{CH}_2 - \text{CH}_2 \end{array} \longrightarrow [\text{-CH}_2 - \text{CH}_2 - \text{O-}]_n \qquad (9)$$

The cationic polymerization employed for this project is suspected to proceed through a mechanism similar to the one described in Fig 1 (see next page).

The use of CF_3SO_3H as an initiator results in the initial ring cleavage, followed by oxonium ion formation. Depending on the statistics of the ring closure versus propagation, crown ethers can be formed, or high polymers can result from the intermolecular counterpart.

Fig. 1 Cationic Polymerization

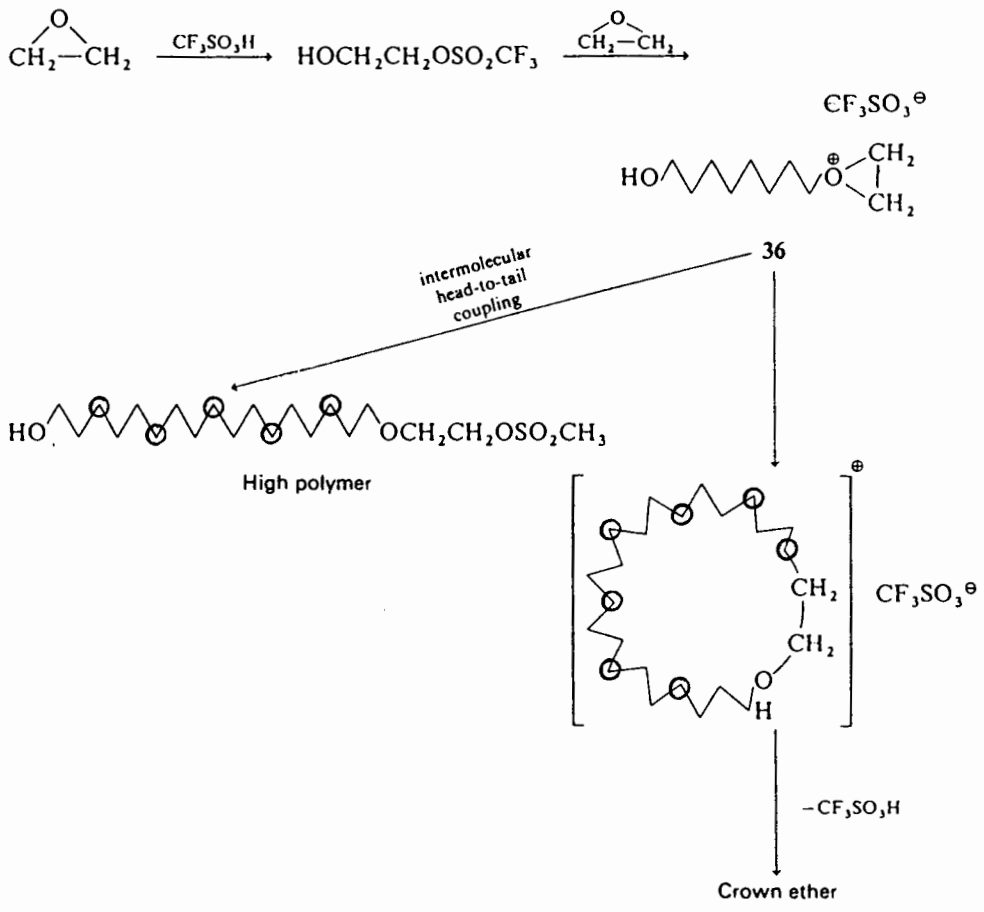

Catalysts

As mentioned earlier, the cationic polymerization is initiated by Lewis acids or Bronsted acids - that means that the photoinitiation requires photochemicals that produce these species. Lewis acids are produced by aryldiazonium salts upon photolysis.

$$Ar\text{-}N_2^+BF_4^- \xrightarrow{h\nu} ArF + N_2 + BF_3 \qquad (10)$$

It was Fischer who introduced aryldiazonium salts into the UV-curing of epoxy resins [18]. Schlesinger [19] was the one to prepare diazonium salts with an extended spectral range. (See Fig. 2). Schlesinger was able to polymerize various mono- and bifunctional epoxy monomers, furanes, dioxycyclopentadiene, oxycyclohexane as well as oligomers and epoxidized novolacs.

Fig. 2 Absorption maxima of aromatic diazonium salts with aryl moieties as indicated. The principal mercury lines are marked on the wavelength axis [19].

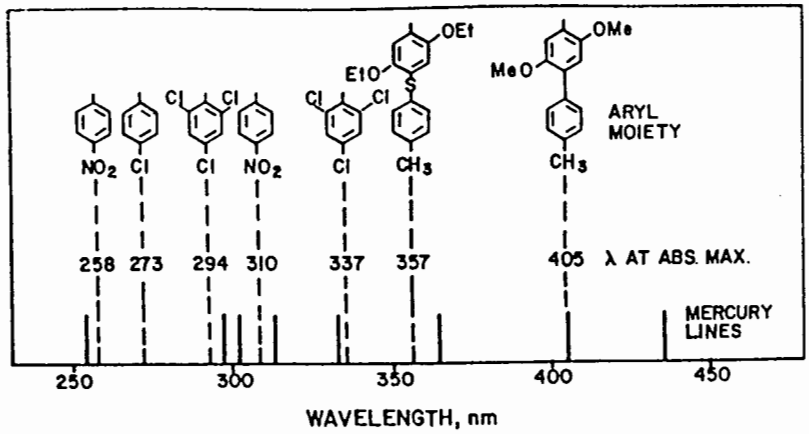

The serious disadvantage of the diazonium salts is their short life-time. The solutions have to be mixed immediately before the reaction. Since this is inconvenient, diazonium salts were replaced by iodonium and sulfonium salts.

New Catalysts

These 'new salts' are easier to handle since they are crystalline, stable and colorless. They can be dissolved in common solvents and in many cationically polymerizable monomers.

Table 3 shows a selection of the large number of onium salts that were prepared by Crivello and Lam [20, 21].

Table 3 Several onium salts

Cations	Anions
R = H, CH3, CH3O, isopropyl, tertbutyl, Cl, Br	BF4-
(R-Ph)2-I+	PF6-
(R-Ph)3-S+	AsF6-
	SbF6-
	SnCl3+

The diaryliodonium and triarylsulfonium salts show a photolysis that is different from the diazonium systems. The photolysis of the iodonium salt is described by the following mechanism [70]

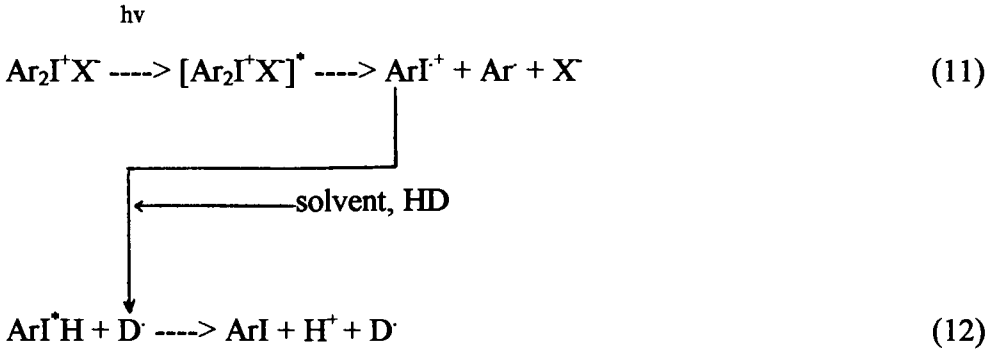

Triarylsulfonium salts behave in a similar fashion:

$$Ar_3S^+X^- + HD \text{ ----> } Ar_2S + H^+ + D^{\cdot} + Ar^{\cdot} + X^- \qquad (13)$$

That this is in fact the mechanism that takes place during photolysis can be easily proved, because no aromatic components become incorporated into the polymer during polymerization. If fluorinated anions are used, none are among the photoproducts. Thus, complex anions survive photolysis intact and no strong Lewis acids are produced. Instead, the corresponding Bronsted acids ($H^+BF_4^-$ or $H^+PF_6^-$) are produced. These acids initiate the cationic polymerization by the action of the proton on the epoxy monomer:

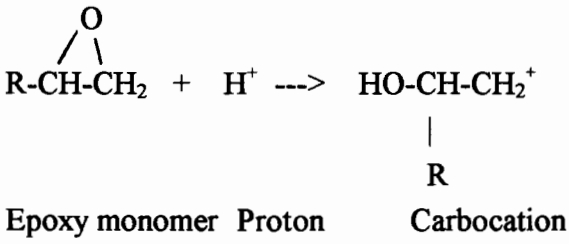

(14)

The complex ions do play an important role in the rate of polymerization. Figure 3 illustrates the difference in rate with different ions [20]. A reason for this observation might be the change in bonding-strength of the proton. In a nonaqueous medium, the proton is bound to the anion, forming an ion-pair. This binding decreases with increasing size of the anion, thus making the proton more easily available and thus more catalytic.

Fig. 3 Photoinitiated polymerization of cyclohexene oxide, with diphenyliodonium salts (0.02 M), the anions of which are indicated in the figure [20]

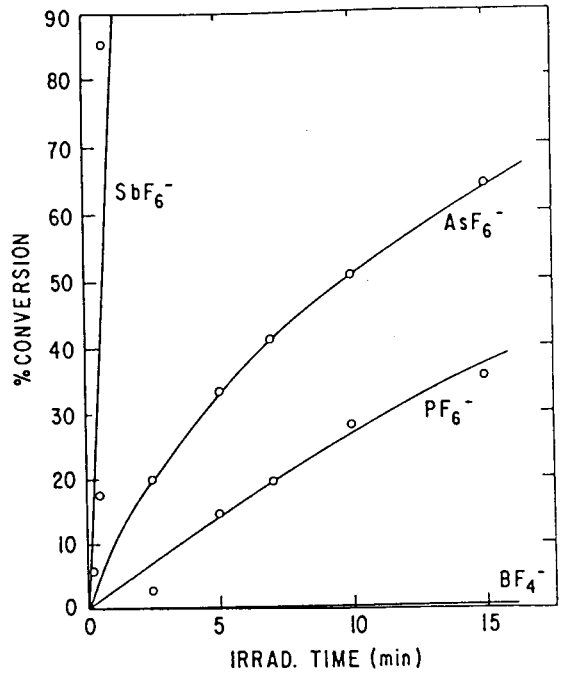

Other initiators of interest:

1. Dialkylphenacylsulfonium salts

If a polymerization is taking place without a terminator, it will not stop after irradiation is over. In fact, it will continue until most of the monomer is consumed. This phenomenon might be of advantage in UV curing, but can be very harmful in imaging applications, where resolution and sharpness can be hurt. Crivello and Lam developed a new species of initiatiators to solve this problem: dialkylphenacylsulfonium salts and the dialkyl-4-hydroxyphenyl sulfonium salts [21, 23, 24]. The photolysis of triarylsulfonium

ions decomposes the initiator, but the photolysis of the new initiators that Crivello and Lam developed does not decompose the initiator.

A photostationary state is formed upon irradiation, as soon as the irradiation stops, the ylid and the Bronsted acid revert to the original sulfonium salt.

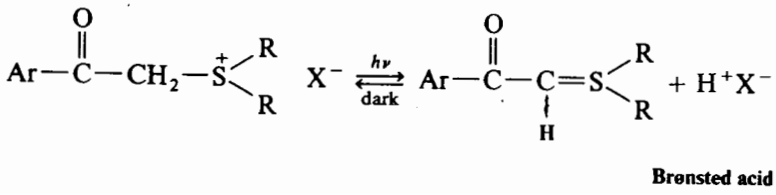

(15)

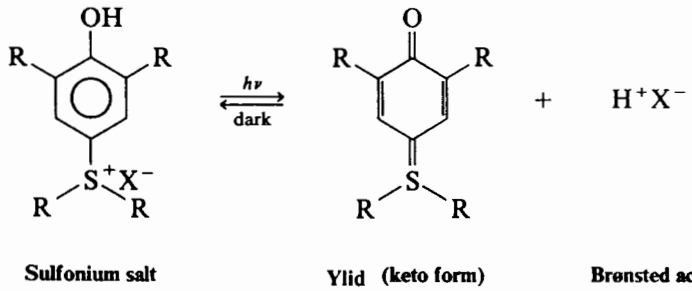

(16)

2. Iron-Arene Complexes

Zweifel and coworkers [25, 26] developed a new class of initiators, which are ferrocenelike iron-arene complexes.

If these initiators get irradiated, they undergo a ligand exchange reaction where the tridentate arene is replaced eventually by the oxygen atom of the epoxy groups [76].

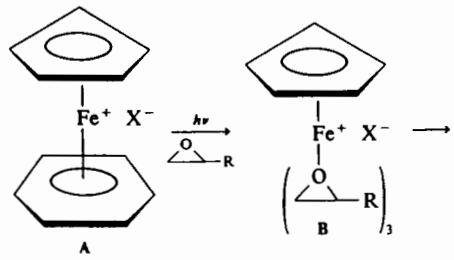

(17)

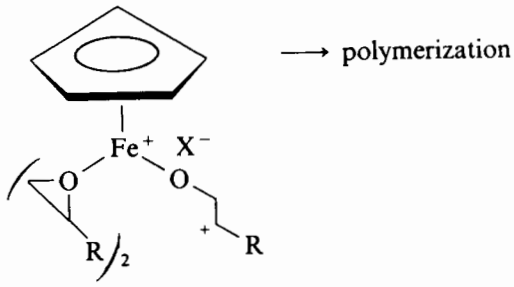

⟶ polymerization (18)

The iron-arenes are less effective initiators of cationic polymerization than the sulfonium salts for example. However, they are still of practical interest because of their stability and the stability of the cured images against degradation.

Curing of epoxides is a two-step process with these inhibitors: they are capable of initiating the cationic chain, but the polymerization process needs thermal activation to proceed.

INTRODUCTION TO THIS STUDY

The enrichment of a polymer surface involves a non-stoichiometric amount of a polymer component at the surface of a polymer film. This amount is disproportionate to the bulk composition.

The enrichment of surfaces is interesting, because the surface of a polymer can be very different from the bulk composition. These surface phenomena are often due to the mobile nature of a polymer. The polymer chains exhibit relaxation processes and cause surface and bulk remodeling. Surface enrichment in this sense is driven by thermodynamics and controlled kinetically. It is determined by the bulk structure of the polymer, the miscibility of its components and the differences in surface free energy between the polymer blocks [37]. Several studies have documented the polymer surface rearrangement that result from the segmental responses to changing external environments (for example from aqueous to air) [39-52].

The low surface free energy of perfluorinated chains is known to enrich the interfaces of polymers [36,53,54]. This phenomenon is interesting and technologically attractive: inexpensive bulk aliphatic polymer resins that are 'doped' with small amounts of expensive fluorinated epoxides can form polymeric fluorinated surface overlayers that exhibit large differences in chemical and physical characteristics from the bulk polymer.

The polar contributions of hydroxyl and sulfonyl fluoride groups reduce the aqueous contact angles. The surface enrichment of the perfluorocomponents is common where the restructuring of the surface allows the film components to rearrange [36,53,54]. Here, the perfluorinated monomers have the lowest interfacial tension with air, and occupy the interfaces in the mixture cast onto glass plates or brass, but prior to film polymerization, causing the difference in characteristics of bulk and surface region.

There is interest in the use of fluorocarbon sulfonyl fluorides as new surfactants, ion-exchange resins, precursors for sulfonic acids [55-58], and as low-refractive index materials; the photo-initiated polymerization of these monomers into polymer films should make possible some interesting applications.

The reaction that takes place is assumed to be the following [63]:

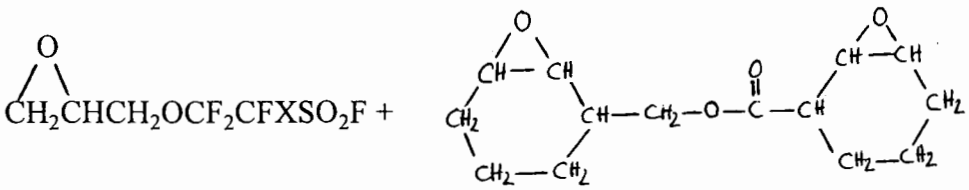

(19)

X = F, CF_3

INSTRUMENTATION

Photopolymerization

The photoinitiated polymerization system was equipped with a 450 Watt Hanovia mercury lamp (or 200 Watt lamp where indicated). The lamp was cooled by water and mounted horizontal under a parabolic aluminum reflector. Both lamp and reflector were put in position in a box.

The distance from the irradiated samples to the center axis of the lamp was 10 inches.

See Figure 4

Fig. 4 Portland State University photo-polymerization system

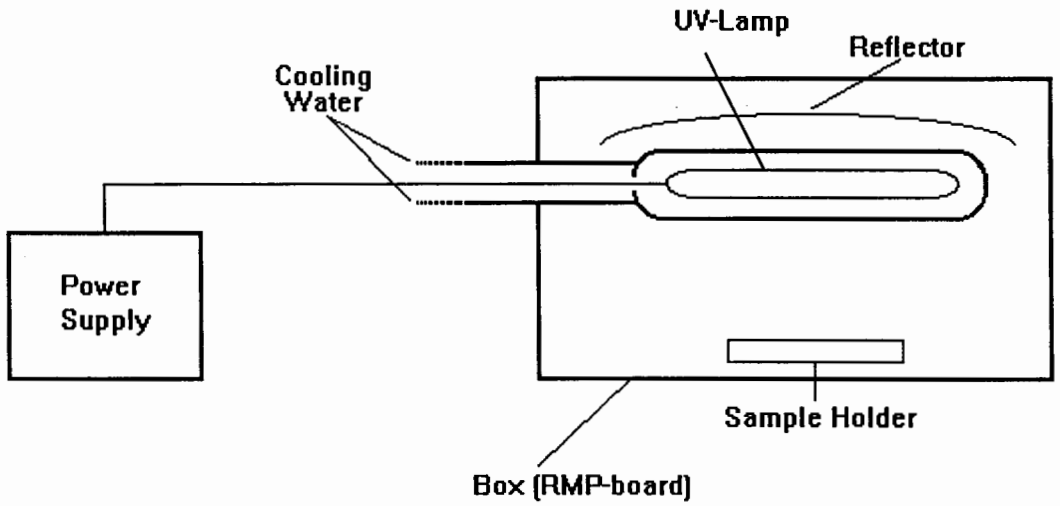

IR System, Portland State University

The spectra were obtained on KBr pellets for liquids and solids. Gas spectra were acquired using a 10 cm path length Pyrex cell fitted with a Kontes Teflon high vacuum stopcock and KBr windows. The spectrometer used was a Nicolet 20 DX, and the spectra were recorded in the range from 4600-400 cm^{-1}. The resolution of this instrument is 2.0 cm^{-1}.

IR System, Colorado State University [28]

Attenuated total reflectance FTIR spectra were collected on a Nicolet 60SX instrument with a liquid N_2 cooled MCT detector using a spectratech variable angle ATR accessory at normal incident angle onto a KRS-5 crystal (50 mm x 10 mm, faces angles = 45^{O}). Bare substrates were used as references. Films on substrates or bare substrates were pressed against the ATR prism to maximize interfacial contact. Spectra were taken at 4 cm^{-1} resolution with 1024 scans. Reference subtraction and flattening were achieved using Spectracalc software (Galactic Industries), but no curve smoothing or other alterations were used.

Photoelectron Spectroscopy, University of Washington [28]

X-ray photoelectron spectroscopy (XPS) were performed on a Surface Science SSX-100 spectrometer (Mountain View, CA) equipped with a monochromatic Al K_{α} source, hemispherical analyzer, and a multichannel detector. Typically, spectra were collected with the analyzer at 55^{O} with reference to the sample surface normal, and the operating voltage was 50 eV using a 1000 μ m spot size. Both survey spectra and data for quantitative analysis were collected at a pass energy of 150 eV and a spot size of

1000 μ m. The binding energy (BE) scales for all spectra were referenced to the C1s C-H peak at 285.00 eV. Peak fitting of the high resolution spectra was done using Gaussian peak shapes with commercial software supplied by Surface Science Instruments. For calculation of XPS elemental composition, the analyzer transmission function was assumed not to vary with photoelectron kinetic energy (KE) [29], the photoelectron escape depth was assumed to vary as $KE^{0.7}$ [29], and Scofields photoionization cross sections were used [30].

Angle-dependent XPS data were collected at nominal photoelectron take-off angles of 0^{O}, 55^{O} and 80^{O}. The take-off angle was defined as the angle between the surface normal and the axis of the analyzer lens system. Using mean free paths calculated from the equations given by Seah and Dench [31], the sampling depth (three times the mean free path) should decrease from 90 Å as take-off angle increases from 0^{O} to 80^{O}.

Introduction to the theory of Photoelectron Spectroscopy

Photoelectron spectroscopy, or XPS involves the analysis of the energy of electrons that are ejected from a sample by incident radiation. XPS allows the investigation of electron structure, and provides a picture of molecular orbitals and core-level binding energies for solids. The energy of the ejected electrons are characteristic and allow elemental analysis and chemical state identification. Photoelectron spectroscopy probes only the surface region, and is frequently used in investigating phenomena such as absorption, corrosion, catalysis, and adhesion - all areas where the surface is of great importance.

The measurements are made of the energy of the ejected electrons. The sample is excited by irradiating with a beam of X-rays, short wavelength UV radiation or electrons.

Three types of electron spectroscopy are encountered. They differ by the way the sample is irradiated.

The most common kind is the X-ray electron spectroscopy. This kind is based upon irradiation with monochromatic X-radiation. It is called XPS or ESCA. The main emphasis in this discussion will be on XPS. The other two types are Auger Electron Spectroscopy, AES, and Ultraviolet Photoelectron Spectroscopy, UPS.

Figure 5 shows a schematic representation of an XPS process.

Fig. 5 Schematic representation of a XPS process

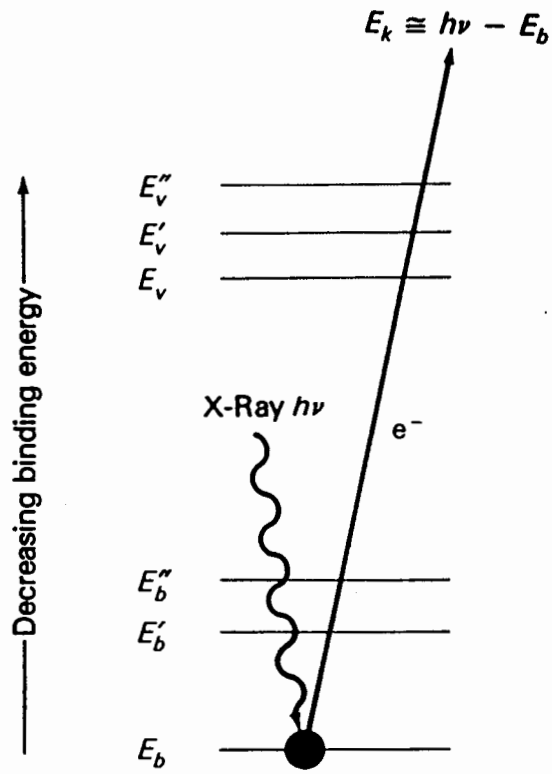

The three lower lines (Eb, Eb' and Eb") represent energies of the inner shell K and L electrons. The upper lines represent some of the energy levels of outer shell or valence electrons. As shown in this figure, one of the photons of the X-ray beam displaces an electron from a K-orbital, or E_b. Only a single electron is ejected.

The reactions that take place are the following:

$$A + hv \rightarrow A^{+*} + e^{-} \qquad (20)$$

A can be an atom or a molecule. A^{+} is an electronically excited ion with a positive charge greater than A. The kinetic energy of the ejected electron is measured in an electron spectrometer.

The energy of the X-ray is known, so it is possible to calculate the binding energy of the ejected electron:

$$E_{hv} = E_b + E_k \qquad (21)$$

$$E_b = E_{hv} - E_k \qquad (22)$$

Every spectrometer also has a 'workfunction' that has to be taken into account. The workfunction is a factor that corrects for the electrostatic environment in which the electron is formed and measured. The workfunction of a spectrometer is the energy necessary to remove an electron from the surface of a spectrometer. This can be understood by tracing through an XPS experiment. An electron is ejected from the sample

with a certain energy, E_l. The electron has to go through the entrance slit of the spectrometer. Since the workfunction of the sample and the spectrometer are different, the kinetic energy of the electron changes to E_K upon entering the spectrometer. This is because the ejected electron is either accelerated or decelerated to the entrance slit. The energy E_K is the energy that is measured. Thus, the workfunction E_w enters the equation.

$$E_b = E_{hv} - E_k - E_w \qquad (23)$$

A 'normal' spectrum of a photoelectron spectrometer is shown in figure 6.

Fig. 6 XPS Spectra of $(C_3H_7)N^+S_2PF_2^-$

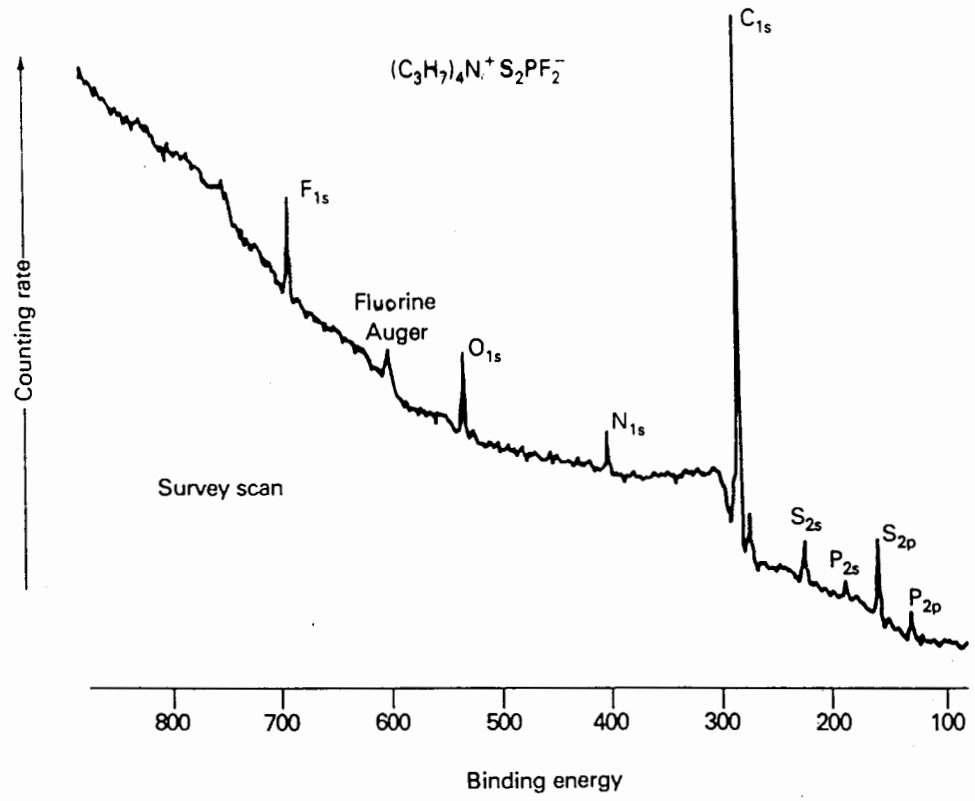

Plotted is the count of the electron rate as a function of the binding energy. The peaks of this organic sample are all well-separated with the exception of hydrogen. In addition, an oxygen peak was detected meaning that surface oxidation or hydrolysis of the sample occurred. It is also shown that the binding energies of 1s electrons increases with increasing atomic number. This is due to the increased positive charge of the nucleus; Z effective increases while n stays the same.

Figure 7 shows a typical photoelectron spectrometer. Electron spectrometers are made up of components whose functions are analogous to those encountered in optical spectroscopic instruments. These components include: a source, sample holder or container, an analyzer, a detector, a signal processor and a readout. The sample holder and source form an integral unit. The source or excitation device consists of an X-ray tube that usually employs Mg or Al targets. K alpha lines have considerably narrower bandwidths than those with higher atomic number targets. Narrow bandwidths are desirable because they lead to enhanced resolution. In the sample compartment, solid samples are mounted in fixed positions as close as possible to the photon source and the entrance slit of the spectrometer as possible. In order to avoid attenuation of the electron beam, the sample compartment must be evacuated to a pressure of 10^{-5} torr or smaller. Often, even better vacuums of 10^{-9} or 10^{-10} torr are required to avoid contamination of the sample surface by substances such as oxygen and water.

Figure 7 Schematic of an electron spectrometer

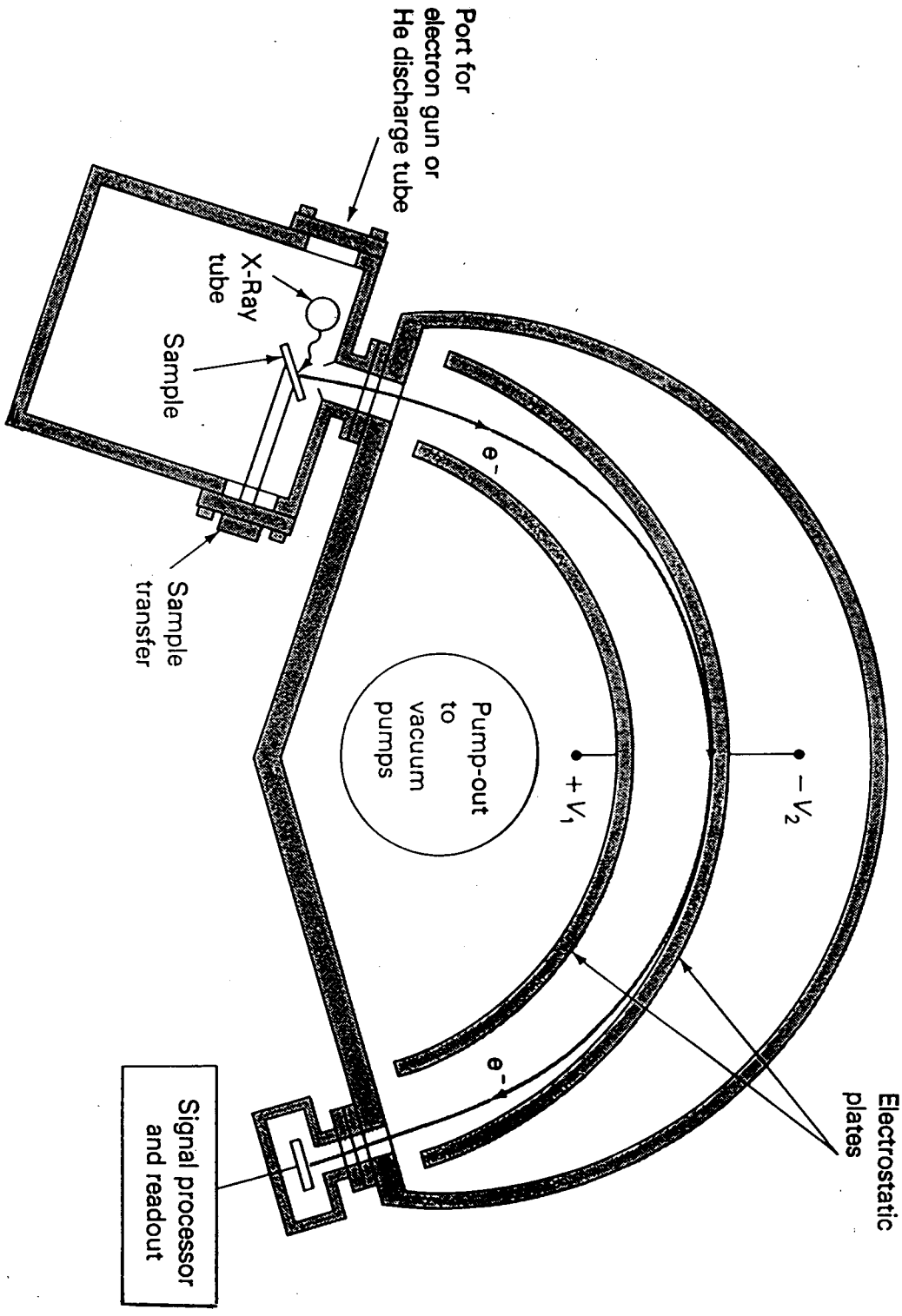

Gas samples are leaked into the sample detection area through a slit of the size that provides a pressure of 10^{-2} torr. The signal is weakened if the pressure is too low.

The most common type of analyzer is the dispersion analyzer. Here, the electron beam is deflected by an electrostatic field. This is done in such a way that the electrons travel in a curved path. The radius of curvature is dependent upon E_K of the ejected electron and the magnitude of the field. By varying the field, electrons of various kinetic energies can be focused on the detector. The deflection plates may be cylindrical, spherical or hemispherical. The pressure in the analyzer is typically maintained at or below 10^{-5} torr.

The detectors in the most modern electron spectrometers are based upon solid state channel electron multipliers. They consist of tubes of glass that have been doped with lead or vanadium. When a potential of several kilovolts is applied across these materials, a cascade or pulse of 10^6 to 10^8 electrons is produced for each incident electron. The resulting pulses are then counted electronically.

Quadrupole Static Secondary Ion Mass Spectrometry [28]

Static secondary ion mass spectroscopy (SIMS) experiments were performed with a Physical Electronics 3700 SIMS system (PHI Electronics, Eden Prairie, MN) mounted on a custom ultrahigh vacuum (UHV) system. The ion beam was rastered over a 5x5 mm area, and the total exposure time of the sample to the ion beam, including setup and data acquisition, was less then seven minutes. Corresponding total ion doses per sample ($< 5 \times 10^{12}$ ions/cm^2) are within the generally accepted limit for static SIMS conditions for organic surfaces[32]. Both positive and negative secondary ions were collected over a m/z range of 0 to 300 with a nominal mass resolution of unity. Data acquisition and control of the energy filter and quadrupole used the Physical Electronics SIMS software package.

The UHV system has a turbomolecular and Ti sublimation pumped analysis chamber with an Θ sample manipulator. The base pressure in this chamber is 1×10^{-10} torr. Samples are transferred into the analysis chamber from a turbomolecular-pumped sample introduction chamber. The PHI SIMS system contains a 90^{O} adjustable energy filter and Balzers 0-511 amu quadruple mass spectrometer for detection of positive and negative secondary ions emitted by the sample. A differentially-pumped Leybold-Heraeus (Koeln, Germany) ion source was used to produce a 0.5 nÅ, 3.5 keV Xe^+ primary ion beam.

Contact Angle Analysis [28]

Sessile drop contact angle analysis (Rame-Hart 100 apparatus) used purified (Millipore 18 MΩ cm resisitivity) water drops (2 μ l) on three separate spots on each film surface in a controlled environment (100 % RH). Measurements were taken on both sides of water drops at ambient temperature 30-40 seconds after drops were applied to

surfaces. Contact angle data report the average of three drops at different surface locations.

EXPERIMENTAL

Apparatus

Vacuum Line [35]

Samples of gases and low-boiling liquids were manipulated by a single manifold that was evacuated by a vacuum pump, operating in conjunction with a liquid nitrogen cold trap. The manifold was made of 25 mm (inside diameter) Pyrex glass tubing fitted with four ports. The ports could be opened or closed with an Eck and Krebs 2 mm high-vacuum stopcock. Vessels or tubing could be attached to a port by means of a 10/30 Pyrex glass standard taper ground glass outer joint. The vacuum was provided by a Welch Duo-Seal rotary pump.

A Frederick Company Televac thermocouple gauge was used to read the pressure in the 1-100 micron range; for the 1 - 760 mm range a mercury manometer was used to measure the pressure. Joints and stopcocks were greased using Fisher Scientific Fluorolube GR-290 or Arthur Thomas' Lubriseal. Halocarbon Corporation's Halocarbon wax was used for connections requiring a wax seal.

Reaction Vessels

Reactions were carried out in Pyrex glass reaction vessels of various sizes to which a Kontes high-vacuum valve with a Pyrex 10/30 standard taper joint was attached. A Teflon magnetic stir bar was used to stir the reaction mixture.

Reagents

The  compound was prepared by N. Robert Holcomb. The

 compound was prepared by the author with the help of N. Robert Holcomb.

From Union Carbide Chemicals and Plastics Company Inc.:

Cyracure UVI-6990 ($Ar_3S^+PF_6^-$), photoinitiator for UV light cured and cycloaliphatic epoxide systems, Cyracure UVR-6110 (3,4-epoxycyclohexylmethyl-3,4-epoxycyclohexylcarboxylate), diepoxide for photopolymerization.

From Airproducts: Liquid Nitrogen, from Aldrich: SO_3.

From DuPont: fuming H_2SO_4, from PCR, Inc. CF_3CFCF_2 and $\overline{OCH_2CHCH_2(CF_2)_8F}$.

From Wacker Siltronic Inc.: Fluoroware Wafer Box, (100 mm) for shipping.

From 3M Specialty Ch. Division: FC-430 - surfactant (assumed to be a C_8 perfluorinated carbon chain with a sulfonyl amide group)

Preparation of the samples and casting of the films

In a typical run, different amounts (e.g., 5, 10 or 17 % by weight) of the fluorinated monomer were mixed with the diepoxide and the photoinitiator (2 % by weight). The chemicals were mixed in a disposable 10 mL plastic beaker. The mixture was stirred using disposable plastic pipettes. Two small drops of the mixture where placed on a substrate (brass or glass) and a film of nominal 10 μ m thickness was cast using a No 10

Meyer rod. The samples were then immediately placed into the UV cavity and irradiated. Some of the samples tested showed contamination with dust and particles. Dr. Grainger suggested a cleaning procedure to prevent contamination. The glass substrates were put into a glass beaker filled with fuming sulfuric acid. They were soaked in that beaker for 12 hours, then rinsed with distilled water and absolute ethanol. The glass substrates were dried under nitrogen atmosphere.

The samples were then heated for the indicated times and irradiated immediately after heating. This cleaning procedure was used starting with experiment number 6.

In a typical run, the following procedure was used:

In a disposable plastic beaker, 5 % (by weight) of the fluorinated monomer are mixed with 93 % of the diepoxide and 2 % of the photoinitiator.

Using disposable plastic pipettes, two drops of the mixture are placed on a precleaned glass plate. The film is cast using a No 10 Meyer rod.

The sample is heated on a hot plate for 30 minutes, placed in its UV cavity and then immediately radiated for 4 minutes.

Synthesis of $\overset{O}{\diagup\diagdown}CH_2CHCH_2O(CF_2)CF(CF_3)SO_2F$ [64]

Approximately 10 g (0.125 mol) of SO_3 are distilled from fuming sulfuric acid and 18.75 g (0.125 mol) of CF_2CFCF_3 were condensed together in a 0.13 L Carius-vessel. The 0.13 l Carius-vessel was warmed to room temperature. The mixture was heated for three days at 105.5 ^{O}C to form $CF_3\overline{CFCF_2OSO_2}$. The yield was 30.21 g. The compound was then distilled and yielded 27.8 g (boiling point 46.5 ^{o}C)

Then 5.05 g of dry AgF was added. The AgF is then heated to 120 ^{O}C for one day after which 8 mL (7.56 g) of diglyme are added. The mixtures are then heated for 2.5 hours to 30-35 ^{O}C after which 3.34 g of epibromohydrin is transferred into the reaction vessel; the mixture is then heated to 30 ^{O}C for four days. The product is washed four times and dried over $MgSO_4$; 52.2% of the product were recovered by distillation (boiling point 115 ^{o}C/90 mm).

The IR spectrum had the following bands (cm $^{-1}$):

1453(vs), 1341 (vs), 1309 (vs), 1261 (vs), 1218 (s), 1108 (s), 1007 (s), 917 (m), 789 (m), 750 (m), 649 (m), 619 (w), 563 (w), 526 (m), 510 (m), 425 (w)

The spectral data agreed with the literature [61].

RESULTS

Four different epoxy compounds were used for this study:

Compound I: 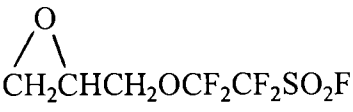

Compound II: 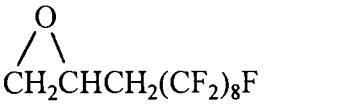

Compound III: 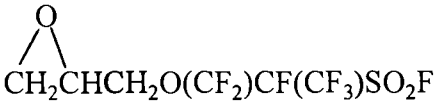

Compound IV: 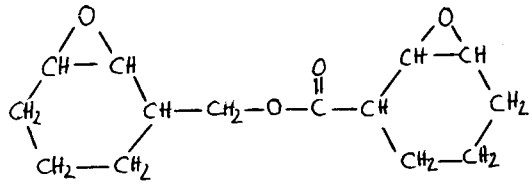

Photoinitiator: $Ar_3S^+PF_6^-$: 2 % by weight; constant percentage for all runs

Nonionic surfactant: $R_FSO_2N(R)CH_2CH_2O(CH_2CH_2O)_mH$; $R_f = C_8F_{17}$-

Explanation for reading the tables:

The amounts of the different compounds used for polymerization are listed in percent weight. The amount of the photoinitiator was held constant at 2 % wt and is not listed in the tables. The results of the quantitative photoelectron spectroscopy are relative abundance data based on percent of total atoms present (not their atomic weight).

Photoelectron spectroscopy does not detect hydrogen, all abundance data is based on all atoms excluding hydrogen.

The surface enrichment factor (SE) for fluorine and sulfur is calculated by dividing the actual amount of fluorine detected (or sulfur, respectively) by the theoretical value expected for the amount of compound I, II or III used (no surface enrichment and evenly distributed compounds assumed). The result is multiplied by 100 to achieve percent.

$$\text{Surface Enrichment (SE-Factor)} = \frac{Concentration\_of\_F\_or\_S\_Detected}{Theoretical\_Concentration\_of\_F\_or\_S} \; x100$$

Introducing a Phosphorous containing photoinitiator

In experiments performed by Dr. Nick Hamel, compound I was copolymerized with a photo-initiator containing SbF_6^-. Antimony shows two peaks in a XPS-spectrum, and one of the antimony peaks interferes with the fluorine peak [28]. In this experiment, a photo-initiator that contains PF_6^- instead of SbF_6^- was used for initiation.

This experiment was repeated twice to determine if results are reliable, radiation times are 4 min.

Table 4 Quantitative XPS analysis of films derived by polymerization of compounds I and IV

	Composition (% wt)		XPS-Values				Theoretical Values				Surface Enrichment (%)	
Sample	I	IV	F	C	O	S	F	C	O	S	F - SE	S - SE
A	65.70	32.40	30.90	37.90	25.10	5.20	20.32	50.68	24.93	4.06	152	128
B	58.80	39.20	33.30	34.30	25.90	5.90	17.87	53.95	24.60	3.57	186	165
C	49.00	49.00	32.80	34.50	26.20	6.00	14.51	58.44	24.16	2.90	226	207
D	32.40	65.70	32.60	34.80	25.90	6.10	9.18	65.54	23.45	1.84	355	332
E	16.70	81.40	31.30	36.90	25.80	5.60	4.55	71.71	22.83	0.91	688	616
F	0.00	98.00	3.80	72.50	23.10	0.40	0.00	77.78	22.22	0.00		
Theory	98.00	0.00										
Theory	0.00	98.00										

Results:

Sample B, C, D (corresponding to approximately 60, 50 and 33 % weight of compound I have essentially identical XPS elemental compositions. The XPS composition is within the range expected for the pure sulfonyl fluoride monomer. This leads to the conclusion that compound I forms a layer of SO_2F groups that is at least as

thick as the sampling depth determined by the XPS-Spectrometer. The surface enrichment seems to increase with decreasing amount of compound I in the sample (surface enrichment factors for fluorine and sulfur increase with decreasing amount of compound I) and is thus highest for the sample with the least amount of compound I. Bromine is detected in all samples that contain compound I and probably originates from the synthesis of this chemical.

Sample E was further investigated using differing sample depths (see table 5)

Table 5 Depth dependent quantitative XPS analysis of a film composed of 16.7 % wt of compound I and 81.4 % wt of compound IV

			Composition (% wt)		XPS-Values				Theoretical Values				Surface Enrichment (%)	
Sample	Take-off angle (o)	Sampl-ing depth (A)	I	IV	F	C	O	S	F	C	O	S	F - SE	S - SE
E	80.00	15.00	16.70	81.40	35.10	32.20	25.60	7.10	4.55	71.71	22.83	0.91	772	780
E	55.00	50.00	16.70	81.40	31.10	38.10	25.20	5.60	4.55	71.71	22.83	0.91	684	616
E	0.00	90.00	16.70	81.40	26.90	43.10	25.70	6.70	4.55	71.71	22.83	0.91	591	736
Theory	55.00	50.00	98.00	0.00										
Theory	55.00	50.00	0.00	98.00										

Results:

The amount of fluorine and sulfur detected on the surface of this sample are much higher then what would be expected from a sample that contains 16. 7 % wt of compound I (surface enrichment factors for fluorine and sulfur are much higher than 100%). The

surface enrichment decreases with increasing sampling depth, and thus supports the theory of surface enrichment of compound I.

No bromine or chlorine were detected in this measurement.

Another set of samples with compound I was run to confirm these results. Unfortunately, the only material left to use was old (samples older than the previously described samples) and the results were not as promising as the results obtained with the newer material (see table 6).

Table 6 Quantitative XPS analysis of films derived by polymerization of compound I and IV, second trial

	Composition (% wt)		XPS-Values				Theoretical Values				Surface Enrichment (%)	
Sample	I	IV	F	C	O	S	F	C	O	S	F - SE	S - SE
I-A	65.70	32.40	6.80	66.70	25.70	0.90	20.32	50.68	24.93	4.06	*	*
I-B	58.80	39.20	6.70	67.40	25.00	0.90	17.87	53.95	24.60	3.57	*	*
I-C	49.00	49.00	6.80	67.00	25.40	0.90	14.51	58.44	24.16	2.90	*	*
I-D	32.40	65.70	4.30	71.00	24.30	0.50	9.18	65.54	23.45	1.84	*	*
I-E	16.70	81.40	3.10	73.30	23.30	0.30	4.55	71.71	22.83	0.91	*	*
I-F	0.00	98.00	0.40	77.80	21.80	0.00	0.00	77.78	22.22	0.00		
Theory	98.00	0.00										
Theory	0.00	98.00										

*no surface enrichment found

Results:

Samples A through C show essentially the same composition. These films do not show any surface enrichment. In fact, the amount of fluorine and sulfur found on the surface is lower than what would be expected from an evenly distributed mixture of

compound I and IV. This trial was run with an old batch of compound I and may explain the inconsistent result. A new batch of compound I was prepared for further experiments.

Introduction of the long-chain compound II

This long chain compound was run with the same composition as listed in experiment one (Table 4). Due to the long, hydrophobic chain of the compound, strong phase separation took place, and made an analysis impossible. Thus, the concentration of this compound was held much lower in the following experiments; improving the mixing of the compounds slightly.

The radiation time was 20 min. (see table 7)

Table 7 Quantitative XPS analysis of films derived by polymerization of compound II and IV, first trial

	Composition (% wt)		XPS-Values			Theoretical Values			Surface Enrichment (%)
Sample	II	IV	F	C	O	F	C	O	F - SE
II-A	4.90	93.10	6.50	67.30	18.70	2.35	76.18	21.47	277
II-B	2.50	95.50	4.10	72.00	23.90	1.19	76.97	21.84	345
II-C	0.90	97.10	4.60	72.60	22.30	0.43	77.49	22.09	1070
II-D	0.50	97.50	1.40	75.50	23.10	0.24	77.62	22.15	583
Theory	98.00	0.00				58.62	37.93	3.45	0.00
Theory	0.00	98.00				0.00	77.78	22.22	

Results:

Surface enrichment is found. The amount of fluorine found on the surface is much lower than that for a pure overlayer of compound II, but much higher than what would be expected for an even distribution of compounds II and IV. An interesting fact is found that with a decreasing amount of compound II, the surface enrichment factor increases. The same phenomenon was found in trial one employing compound I.

Sample II-A was contaminated with 2.5 % copper, 4.7 % zinc, and 0.4 % lead. The source of these heavy metals is unknown. Sample II-C is contaminated with 0.5 % sodium.

Some phase separation remained in all samples.

Use of surfactant to eliminate phase separation

The concentration of surfactant was varied and found to be most effective at 4 percent by weight.

For the following set of experiments, 4 % surfactant were added (see table 8)

Table 8 Quantitative XPS analysis of films derived by polymerization of compound II and IV, employing surfactant to eliminate phase separation.

	Composition (% wt)		XPS-Values				Theoretical Values			Surface Enrichment (%)
Sample	II	IV	F	C	O	N	F	C	O	F - SE
II-E	2.50	91.50	29.20	51.30	16.90	1.40	1.24	76.93	21.82	2346
II-F	0.90	93.10	19.80	57.70	20.50	1.20	0.45	77.47	22.08	4345
II-G	0.50	93.50	29.70	50.30	17.50	1.40	0.25	77.61	22.14	11984
II-H	0.00	94.00	30.50	52.10	14.00	1.80	0.00	77.78	22.22	
Theory	98.00	0.00					58.62	37.93	3.45	
Theory	0.00	98.00					0.00	77.78	22.22	

Results:

Surface enrichment is detected. The amount of fluorine found on the surface is much lower than that for a pure overlayer of compound II, but much higher than what would be expected for an evenly distribution of compound II and IV. An interesting fact is found that with a decreasing amount of compound II, the surface enrichment factor increases. The same phenomenon was found in trial one employing compound I. Up to this point, the different samples seem to show the same results as in the previous experiment employing compound II. However, the last trial (with 0 % wt of compound II) shows the most fluorine enrichment, suggesting that surface enrichment is caused by the surfactant. More experiments need to be performed in order to determine whether compound II or a mixture is responsible for the observed surface enrichment.

Introduction of compound III

Compound III was run with the same procedure as reported for compound I. No phase separation took place. Radiation time: 4 min. (see table 9)

Table 9 Quantitative XPS analysis of films derived from polymerization of compound III and IV, first trial

	Composition (% wt)		XPS-Values				Theoretical Values				Surface Enrichment (%)	
Sample	III	IV	F	C	O	S	F	C	O	S	F - SE	S - SE
III-A	50.00	48.00	8.60	66.10	24.90	0.50	17.32	57.98	22.22	2.46	*	*
III-B	33.00	65.00	11.60	63.40	24.80	0.20	10.94	65.28	22.22	1.70	106	*
III-C	17.00	81.00	5.60	69.40	24.70	0.30	5.42	71.59	22.22	0.92	103	*
Theory	98.00	0.00					38.89	33.33		4.28		
Theory	0.00	98.00										

* no surface enrichment found

Results:

The samples show fluorine concentrations that are lower than what would be expected from and evenly distribution of compound III and IV. No surface enrichment was detected. Contamination with dust and particles may be the reason for this result.

NOTE: In all of the above runs, the glass plates or brass substrates were not cleaned. The rest of the studies were carried out under more controlled conditions with cleaned surfaces, preheating and irradiation in a nitrogen atmosphere.

Further investigation of the three compounds

The glass plates that were used as substrates are now cleaned as described in the experimental section. This proved to be necessary because of the heavy contamination of the samples with dust and particles.

The samples were also preheated under nitrogen in order determine if this would enhance fluorine surface enrichment. The following table shows a study of the newly developed cleaning procedure, using a sample composed of 50 % wt of compound III and 48 % wt of compound IV (see table 10). The glass substrates were cleaned as stated in the experimental section. They were then heated for 30 minutes at 55 ^{o}C under nitrogen.

Table 10 Quantitative XPS analysis of a film derived by polymerization of compound III and IV, employing several different pre-annealing times and different UV-treatments

			Composition (% wt)		XPS-Values				Theoretical Values				Surface Enrichment (%)	
Sample	Pre-heat-ing (h)	UV-Treat-ment	III	IV	F	C	O	S	F	C	O	S	F - SE	S - SE
A	0.50	450W/4 min	50.00	48.00	37.50	34.80	20.80	5.90	17.32	57.98	22.22	2.47	217	238
B	0.50	450W/8 min	50.00	48.00	36.80	35.70	21.00	5.90	17.32	57.98	22.22	2.47	213	238
C	1.00	450W/4 min	50.00	48.00	37.30	34.70	21.20	6.20	17.32	57.98	22.22	2.47	215	251

			Composition (% wt)		XPS-Values				Theoretical Values				Surface Enrichment (%)	
Sample	Pre-heat-ing (h)	UV-Treat-ment	III	IV	F	C	O	S	F	C	O	S	F - SE	S - SE
F	2.00	450W/8 min	50.00	48.00	37.00	35.00	21.30	6.40	17.32	57.98	22.22	2.47	214	259
G	1.00	200W/8 min	50.00	48.00	34.40	32.40	23.40	6.30	17.32	57.98	22.22	2.47	199	255
H	1.00	200W/16min	50.00	48.00	36.50	35.60	21.10	6.10	17.32	57.98	22.22	2.47	211	247
I	3.00	200W/8 min	50.00	48.00	36.50	35.80	20.60	5.90	17.32	57.98	22.22	2.47	211	238
K	3.00	200W/16min	50.00	48.00	37.00	35.40	20.60	6.00	17.32	57.98	22.22	2.47	214	243
Theory			98.00	0.00										
Theory			0.00	98.00										
STDV					0.40	0.40	0.30	0.20						

Results:

All of the samples appear to have essentially the same surface composition. The SE-factors of fluorine and sulfur show surface enrichment consistent for each treatment employed.

IR Spectra

The infrared spectra of samples A through K were similar and had the following bands (cm^{-1}): 3694 (vw), 3620 (vw), 2916 (m), 2850 (m), 1535 (m), 1461 (w), 1402 (w), 989 (m), and 915 (w)

Repetition of experiments using the cleaning procedure

Compound I

The glass substrates were cleaned as stated in the experimental section. They were then heated for 30 minutes at 55 ^{O}C under a nitrogen atmosphere.

Table 11 Quantitative XPS analysis of films derived by polymerization of compound I and IV, third trial

	Composition (% wt)		XPS-Values*				Theoretical Values				Surface Enrichment (%)		
Sample	I	IV	F	C	O	S	F	C	O	S	F - SE	S - SE	Contact Angle
K2	50.00	48.00	27.90	44.80	19.50	3.70	14.84	57.99	24.20	2.97	188	125	62+/-4.7
I2	30.00	68.00	19.60	52.80	23.80	2.80	8.46	66.50	23.35	1.69	232	166	65+/-3.6
H2	17.00	81.00	17.10	55.50	23.60	2.90	4.64	71.59	22.84	0.93	369	313	61+/-4.8
G2	5.00	93.00	12.10	62.50	22.40	2.00	1.33	76.01	22.40	0.27	913	754	62+/-4.5
F2	1.00	97.00	2.40	75.30	21.80	-	0.26	77.43	22.26	0.05	914		61+/-1.1
Theory	98.00	0.00											
Theory	0.00	98.00											

*Values for chlorine, from K2 to F2 were 4.2%, 1.0%, 1.0%, 1.1 %, and 0.5 %.

Results:

Surface enrichment was detected; both fluorine and sulfur show surface enrichment that increases with decreasing amount of compound I. The surface enrichment is lower than what would be expected from a pure overlayer of compound I.

IR Spectra:

The infrared spectra of samples F2-K2 were similar and had the following bands (cm^{-1}): 3694 (vw), 3620 (vw), 2916 (m), 2850 (m), 1535 (m), 1461 (m), 1402 (w), 1395 (w), 989 (vs), 915 (vs), 824 (vw), and 724 (vw).

Compound III

The glass substrates were cleaned as stated in the experimental section. They were then heated for 30 minutes at 55 ^{o}C under a nitrogen atmosphere.

Table 12 Quantitative XPS analysis of films derived by polymerization of compound III and IV, second trial

	Composition (% wt)		XPS-Values*				Theoretical Values				Surface Enrichment (%)		
Sample	III	IV	F	C	O	S	F	C	O	S	F - SE	S - SE	Contact Angle
A2	50.00	48.00	36.90	35.60	21.30	5.80	17.32	57.98	22.22	2.72	213	213	76+/-4.4
B2	30.00	68.00	37.70	35.20	21.60	5.60	9.87	66.50	22.22	1.66	382	337	70+/-3.2
C2	17.00	81.00	36.00	37.70	21.60	5.10	5.42	71.59	22.22	0.95	665	537	71+/-2.0
D2	5.00	93.00	29.20	43.60	23.20	3.90	1.55	76.01	22.22	0.28	1887	1382	67+/-2.1
E2	1.00	97.00	22.50	51.60	22.80	3.10	0.31	77.43	22.22	0.06	7337	5473	63+/-1.5
Theory	98.00	0.00											
Theory	0.00	98.00											

* For A2, chlorine was found to be 0.5 %.

Results:

These samples show surface enrichment that is lower than what would be expected from a pure overlayer of compound III. The surface enrichment of fluorine and sulfur is high though, and increases with decreasing amount of compound III in the sample. The amount of fluorine and sulfur found in the samples that contain 5 and 1 % wt of compound III almost show the amount of fluorine and sulfur expected from a pure overlayer of compound III.

IR Spectra

The infrared spectra of sample A2-E2 were similar and had the following bands (cm^{-1}): 3694 (vw), 3620 (vw), 2916 (s), 2850 (s), 1535 (vs), 1461 (m), 1402 (w), 989 (vs), and 915 (vs)

Depth dependent XPS analysis for a photopolymerized film containing 1% compound III and 99% Cyracure diepoxide

Table 13 Depth dependent quantitative XPS analysis of a film composed of 1 % wt of compound III and 97 % wt of compound IV

			Composition (% wt)		XPS-Values				Theoretical Values			
Sample	Take-off angle (o)	Sampling depth (A)	III	IV	F	C	O	S	F	C	O	S
E2	80.00	15.00	1.00	97.00	28.40	46.00	21.90	3.80	0.31	77.43	22.22	0.06
E2	55.00	50.00	1.00	97.00	18.20	56.90	22.80	2.10	0.31	77.43	22.22	0.06
E2	0.00	90.00	1.00	97.00	13.00	60.60	23.10	1.40	0.31	77.43	22.22	0.06
Theory	55.00	50.00	98.00	0.00								
Theory	55.00	50.00	0.00	98.00								

Surface Enrichment (%)	
F - SE	S - SE
9261	6709
5935	3708
4239	2472

Results:

A surface enrichment that almost corresponds to a pure overlayer of compound III is found at the shallowest sampling depth, 15 A. Surface enrichment decreases with increasing sampling depth.

Mixture of compound I and III

In sample L2, 2 % by weight of compound III was mixed with 3 % by weight of compound I. The glass substrates were cleaned as stated in the experimental section. They were then heated for 30 minutes at 55 ^{o}C under a nitrogen atmosphere.

Table 14 Quantitative XPS analysis of a film derived from polymerization of 3 % wt of compound I, 2 % wt of compound III and 93 % wt of compound IV

	Composition (% wt)			XPS-Values				Theoretical Values				Surface Enrichment (%)	
Sample	I	III	IV	F	C	O	S	F	C	O	S	F - SE	S - SE
L2	3.00	2.00	93.00	28.80	44.40	23.20	3.30	1.43	76.66	22.52	0.28	2019	1179

Results:

This sample shows surface enrichment that corresponds to a pure overlayer of compound I and III.

IR Spectra

19. Sample L2

The infrared spectrum of this sample had the following bands (cm $^{-1}$):

3694 (vw), 3620 (vw), 2916 (m, 2850 (m), 1535 (m), 1461 (w), 1402 (w), 989 (s), and 915 (s)

DISCUSSION

All three compounds listed as I, II, III are believed to polymerize with the epoxide Cyracure as easily as found for compound I in former studies. The polymerization takes place via photocatalyzed initiation. The easy transformation of viscous liquid monomer mixtures into insoluble robust polymer films supports theory of that theory.

The polymerized films were generally transparent at all monomer compositions - only compound II showed phase separation. Adding surfactant to the monomer mixtures of this compound eliminated that problem.

Compound I

Two sets of results were obtained with compound I. Consistent results were not obtained with this compound. The polymerized films of compound I were analyzed by ATR-FTIR. The films displayed spectral features that are consistent with their chemical structure. The most prominent peaks are: hydroxyl- OH stretch (2^{o} ring-opened alcohol) at 3693 and 3619 cm^{-1}, hydrocarbon asymmetric stretch and symmetric stretch ($-CH_2-$) at 2916 and 2850 cm^{-1}; carbonyl stretch of the ester in aliphatic diepoxide at 1534 cm^{-1} cycloepoxide and sulfone (S=O) asymmetric stretch 1460 cm^{-1} [56], C-O stretch and CF_2 stretching in the region of broad bands near 1000 cm^{-1} and another C-F peak at 914 cm^{-1}. Vibrational bands of sulfonyl fluoride S-F stretching bands are found at 823 cm^{-1} and the S-F band is found at 724 cm^{-1}.

A set of XPS data has been collected for various sample compositions of compound I.:

Figure 8 shows the XPS C_{1s} spectra for the copolymerized films with the following compositions:

F2 - 1% compound I and 97 % epoxide, G2- 5% compound I and 93 % epoxide, H2-17 % compound I and 81 % epoxide, I2 30% compound I and 68% epoxide, K2-50 compound I and 48 % epoxide.

Figure 8 XPS Spectra of $\overline{\text{OCH}_2\text{CH}}\text{CH}_2\text{OCF}_2\text{CF}_2\text{SO}_2\text{F}$

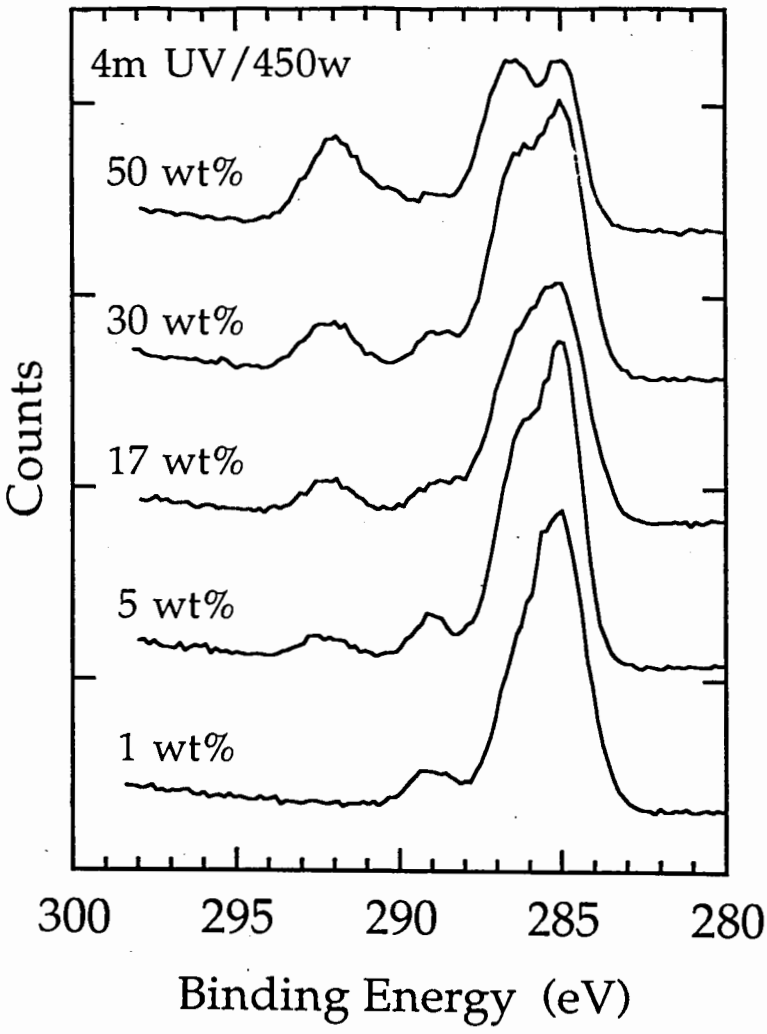

The compositional dependence of the XPS data does not appear to be very strong. With a decrease in the amount of fluorinated monomer I, the characteristic signals for the hydrocarbon epoxide become more dominant. At 1%, no more fluorinated monomer was detected. The surface enrichment with compound I does not seem to be very strong in this case, resulting in less surface overlayer formation. All other film compositions show detectable fluorine surface enrichment. The sample with equal proportions of compound I and the epoxide show a surface that is similar to a film of 100 % wt fluorinated epoxide (Fig 8). Table 4 shows the XPS data for compound I with various concentrations of the diepoxide (compound IV). The elemental compositions (XPS) of the 65.70 , 49.00 and 32.40 % sulfonyl fluoride concentrations are essentially the same. The XPS composition is within experimental error of the value that is expected from a pure sulfonyl fluoride monomer overlayer, thus suggesting that the sulfonyl fluoride forms a layer on the surface, that is at least 50 Å thick. Figure 9 shows the expected peaks. The two major peaks are C-O (BE = 286.5 eV) and CF_2 (BE = 292 eV). The small peak at 285 eV is most probably from a hydrocarbon species, arising from the epoxide or adsorbed CH contaminants on the surface. The binding energy of S $2p_{3/2}$ was 170.3 eV which is higher than the value usually obtained (168 eV) for sulfones in hydrocarbons. This shift is believed to be due to the strong electron withdrawing power of the Fluorine atom attached to the sulfur atom.

The angle dependent XPS results displayed in table 5 show that the elemental XPS composition of compound I is consistent with a pure overlayer of the sulfone monomer at the shallowest sampling depths. With increasing sample depth the composition changes in a way that represents the presence of some epoxide below the surface layer of sulfone monomer.

The data of the contact angle analysis for compound I is shown in table 11. They show decreased aqueous wettability, which is consistent with the overall lower fluorine enrichment seen in these films by the XPS. The wettability is decreased overall if

compared to the pure epoxide [59], thus supporting the presence of at least some fluorinated epoxide in the surface.

Figure 9 XPS Spectra of $\overline{OCH_2CH}CH_2OCF_2CF_2SO_2F$

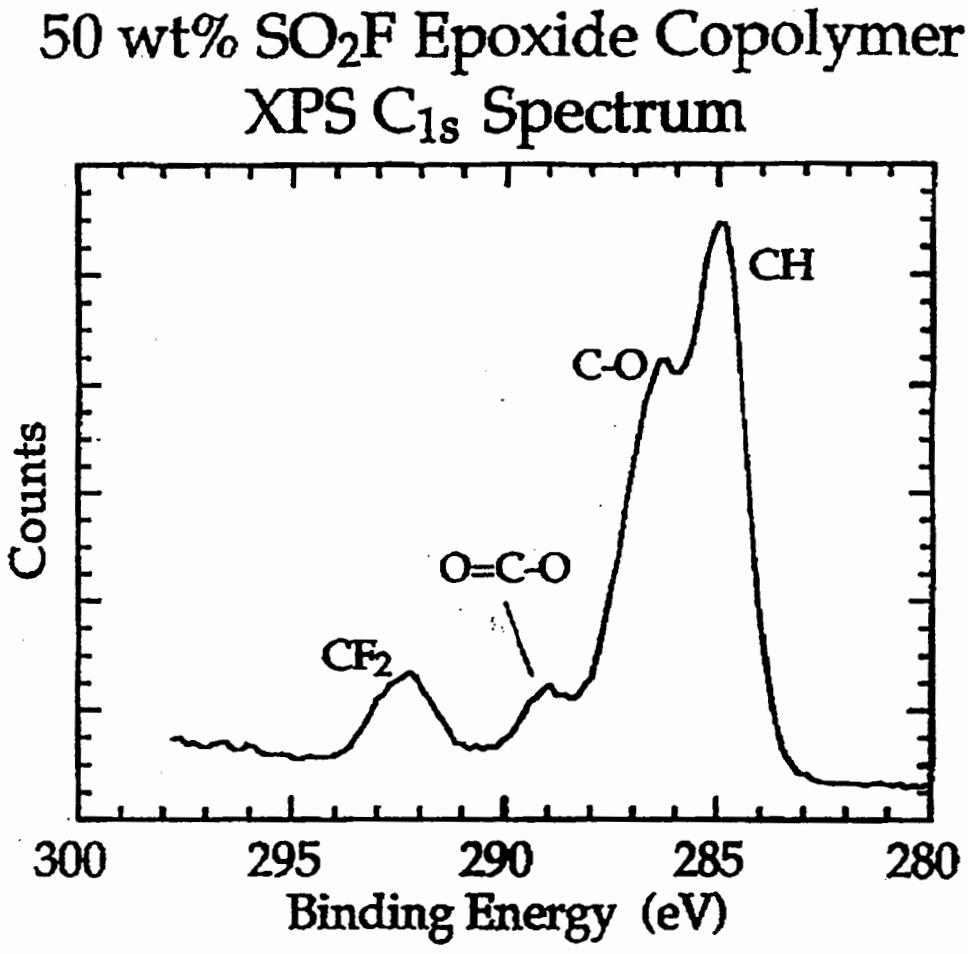

Static SIMS was performed on a film made from compound I (60 % wt) and the diepoxide. Positive and negative secondary ion spectra were obtained; the most informative were the negative ion spectra. Figure 16 shows the representative spectrum. The biggest peaks were found at m/z = 19, 83 and 199. These are consistent with $[F]^-$, $[SO_2]^-$ and $[OCF_2CF_2SO_2F]^-$ fragments from compound I. This is another indication for the presence of this compound at the surface of the copolymer films (the sampling depth of SSIMS is ca. 15 Angstrom). Smaller peaks that were found can also be assigned to fragments of compound I: the peak at m/z = 133 is due to the fragment $[CF_2SO_2F]^-$. The positive ion static SIMS spectra showed primarily peaks of hydrocarbon and fluorocarbon fragments.

Compound II

The long chain compound II shows XPS data that is consistent with what can be expected from the results obtained with compound I. Difficulties were encountered in the beginning due to the hydrophobicity of the long chain. Phase separation took place when the compound was mixed with the diepoxide and the photoinitiator. A surfactant provided by 3M was used to avoid that. At the surfactant concentration of 4% by weight, no more phase separation took place, and the samples could be run without a problem.
XPS data obtained at a low percent by weight (5 %) and less shows some fluorine enrichment in the surface prior to using the surfactant (Table 7). Surface enrichment is lower than what would be expected from a pure overlayer of compound II, however.

Table 8 shows the result after using the surfactant. Fluorine concentrations are almost constant at 29% percent with 2.5%wt of compound II and less. The surfactant is a compound made out of a long, perfluorinated chain and an active polar group. The fluorine content in this experiment was highest in the set that contained 0 % of compound II. This does suggest surface enrichment - however, the enriched substance in this set has

to be the surfactant. The fact that adding compound II does not increase the amount of fluorine detected leads to the assumption that the surfactant forms a layer on the surface, which permits further enrichment with compound II. Further experiments should determine whether the surfactant or compound II or possibly a mixture is favored for surface enrichment.

Compound III

The polymerized films were analyzed by ATR-FTIR. The results are consistent with what would be expected from its chemical structure. The most distinguished peaks are the same found for compound I: hydroxyl- OH stretch (2^{o} ring-opened alcohol) at 3693 and 3619 cm^{-1}, hydrocarbon asymmetric stretch and symmetric stretch ($-CH_2-$) at 2916 and 2850 cm^{-1}; carbonyl stretch of the ester in aliphatic diepoxide at 1534 cm^{-1} cycloepoxide and sulfone (S=O) asymmetric stretch 1460 cm^{-1} [60], C-O stretch and CF_2 stretching in the region of broad bands near 1000 cm^{-1} and another C-F peak at 914 cm^{-1}. The vibrational band for the S-F stretching mode is found at 823 cm^{-1}.

The data for the aqueous contact angle data are shown in table 12. The wetting data indicate relatively hydrophobic surfaces at all film compositions. The values found are different from the value of a film composed of pure cycloaliphatic diepoxide (41^{o} [62]). The values are somewhat reduced by polar contributions from the hydroxyl and sulfonyl fluoride groups, and are thus lower than what otherwise would be expected for a hydrophobic fluorinated polymer [61]. The data are consistent with an overlayer of the fluorinated epoxide exposed to air. The data shows that a hydrophobic fluorinated overlayer persists at the film surface, forming bulk compositions that are enriched in the diepoxide.

Figure 10 shows the XPS spectra for copolymer films of varying composition of compound III. A compositional dependence for the amount of fluorinated polymer used is found. The spectra for films having high percentages of fluorinated epoxide are shown at the top. The features described in figure 16 are prominent down until a percentage of 17 % fluorinated polymer. Then, the chemical features that were associated with the pure diepoxide in the discussion of figure 11 are growing into the spectra of the film made of 17, 5 and 1% wt perfluorinated epoxide. But even so, the CF_3, CF_2 and CF peaks remain strong.

The XPS data shown in Fig 11 displays a C1s spectrum for a copolymer film consistent of 50% compound III and 50% diepoxide. Only little hydrocarbon was found within the sampling depth of 50 Å. The strongest peaks include carbon (287 eV) and several fluorinated species of carbon (C-F, 290 eV; CF_2, 293 eV; CF_3, 294 eV). The perfluorinated carbon signals are strong, hydrocarbon signals are almost non-existing - this suggests high levels of enrichment of perfluorinated species in the upper surface of the film.

Figure 12 shows the spectra for a film that is polymerized by the diepoxide alone. Compared to figure 11, it becomes apparent that the homopolymer film of the diepoxide lacks the fluorocarbon peaks, while the fluorinated polymer lacks the carbonyl peak at 289 eV and the CH_x peak at 285 eV.

Figure 10 XPS Spectra of $\overline{OCH_2CH}CHCH_2O(CF_2)CF(CF_3)SO_2F$

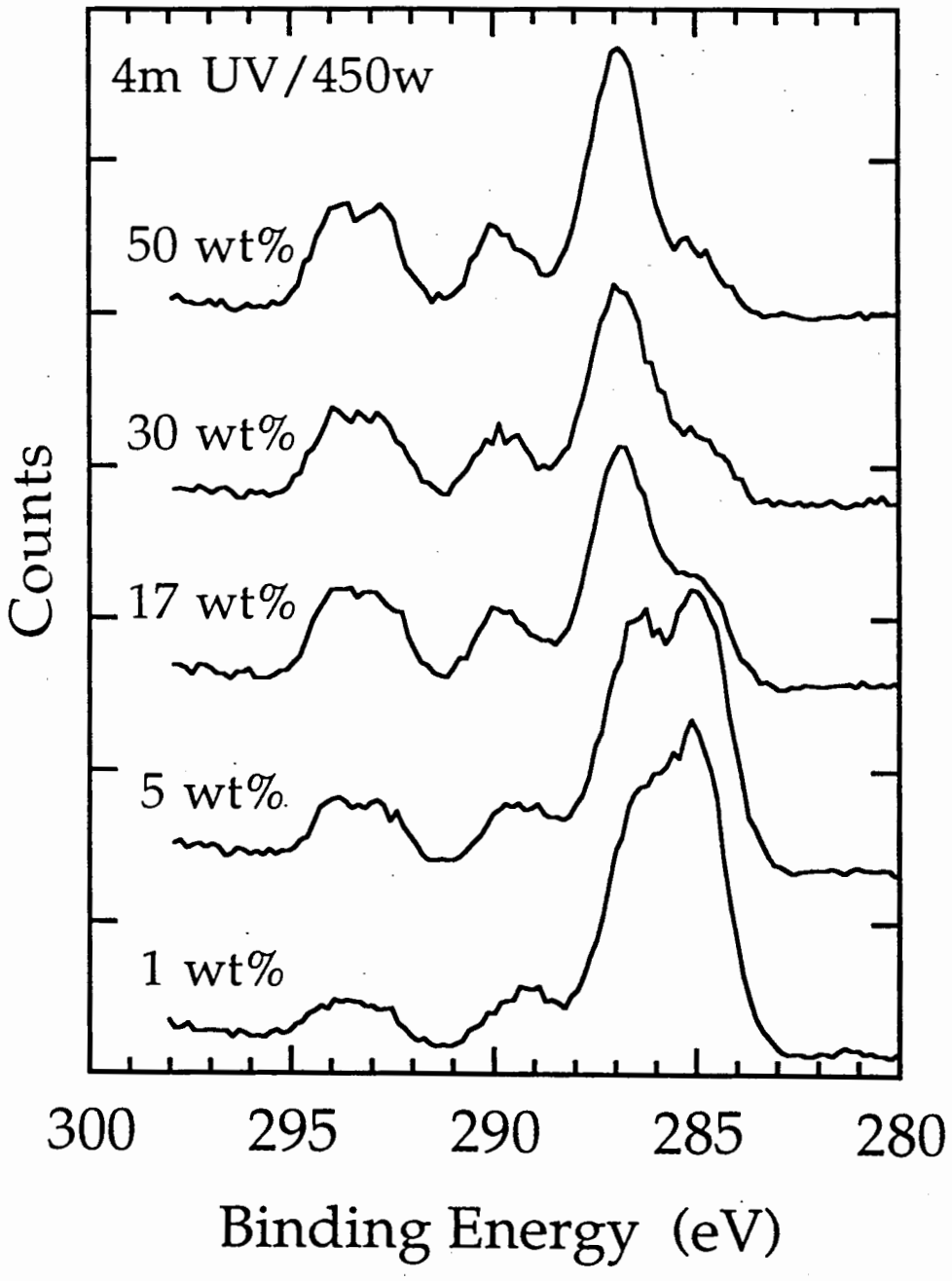

Figure 11 XPS Spectra of compound III (50 % wt)

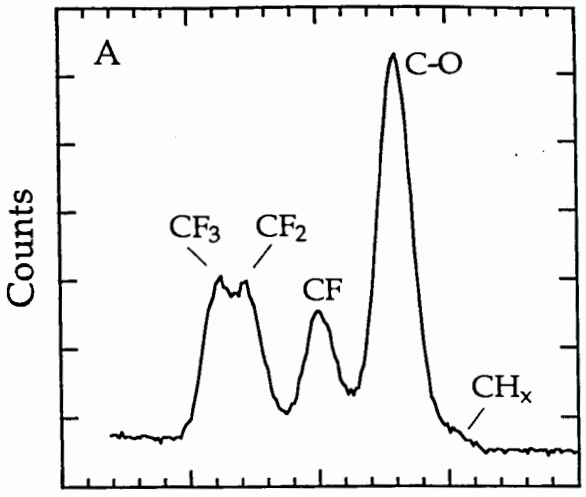

Figure 12 XPS Spectra of compound IV (98 %)

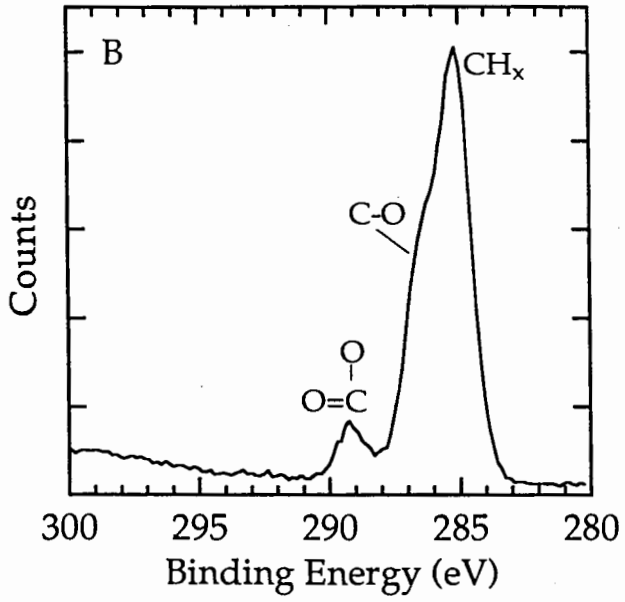

Table 12 shows the compositional data for the films composed of varying amounts of compound III. Comparing the results to the theoretical composition for a film made of 100% wt of compound III, it shows substantial non-stoichiometric increases in sulfur and fluorine content at their surface. Thus, the fluoroepoxide becomes enriched at the surface. The sample depth of the XPS signal is app. 50 Å, so the surface enrichment of compound III extends at least to this depth. It is significant that even with a film composition of 1 % wt of compound III high amounts of fluorine and sulfur are found on the surface.

Another interesting results is that for films containing equal amounts of compound III and the diepoxide (table 10), a pre-polymerization annealing step (55 ^{o}C under nitrogen) ranging from 0.5 to 3 hours, or changing the intensity of the UV-irradiation, or irradiation times of different length does not change the surface composition. This suggests that monomer migration, phase separation and surface enrichment occur fast in cast films before they are polymerized.

Figure 13 shows the results of an angular resolved spectrum for sample E2, using a film of 1% wt fluorinated epoxide; 15 Å, 50 Å and 90 Å sampling depths were studied. The data shows that both fluorine and sulfur species have the highest concentration at the surface of the film. This supports the theory of a gradient of increasing fluoroepoxide content from the bulk to the surface of the film. The depth profile is displayed in figure 13, showing these trends. The profile was calculated from the XPS angle-resolved data using an improved regularization algorithm . The calculated gradient of the fluoroepoxide is shown in this figure. The concentrations of S, F, C and O are very close to the values that would be expected from a 100% monomer at the top of the surface.

Figure 13 Depth dependent XPS Spectra for copolymer E2

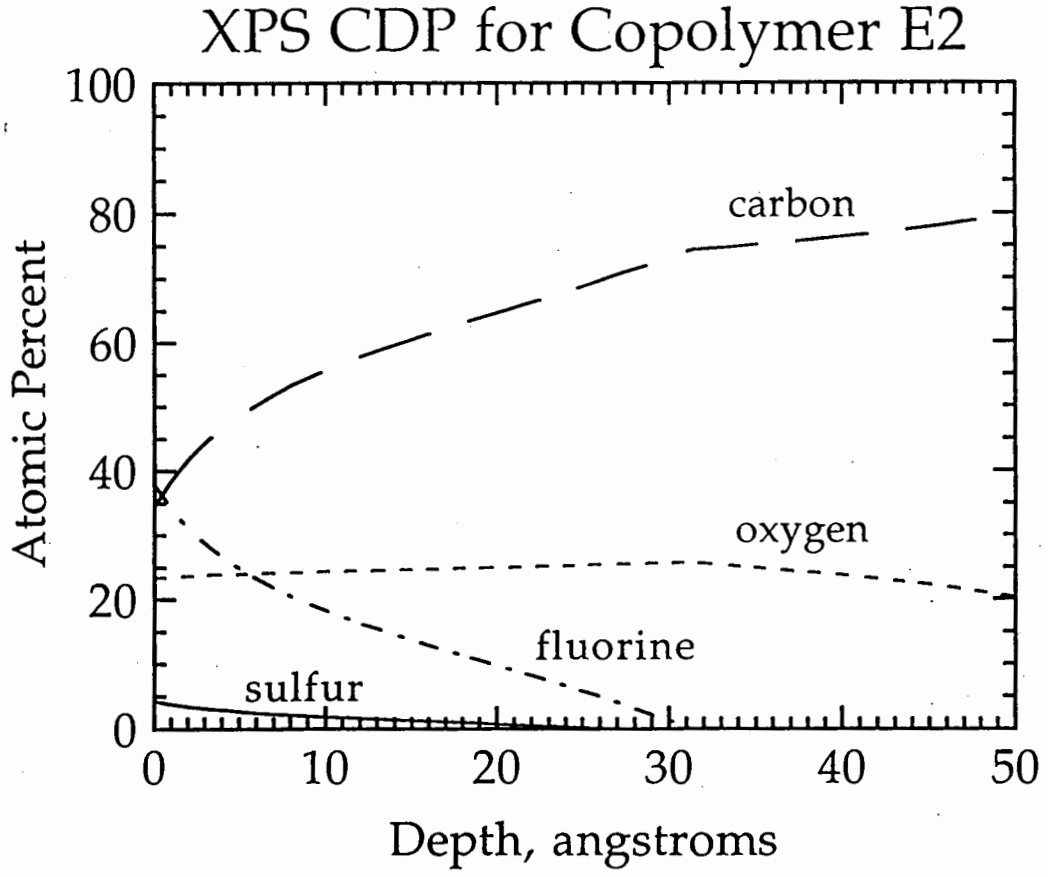

CONCLUSIONS AND RECOMMENDATIONS FOR FURTHER STUDIES

The different methods of surface analysis used for characterizing photo-initiated copolymerized films composed of mixtures of fluorinated sulfonyl fluoride epoxide monomers and the commercial aliphatic diepoxide show that the fluorinated epoxide migrates to the surface of the film-air interface. This triggers a non-stoichiometric enrichment of the film surface with the fluorinated epoxide bearing sulfonyl fluoride groups. The surface segregation effect is more prominent for fluorinated epoxide I and III. These compounds have a perfluorinated carbon chain, a sulfonyl fluoride group and an extra CF_3 group (compound III). The extra fluorocarbon features seem to make surface enrichment easier. The surface enrichment of compound III causes the formation of a prominent fluorinated polymer overlayer in all film compositions down to 1 % wt. This overlayer forms only at the richer compositions of fluoroepoxide I in mixed films. The surface enrichment found in trials employing compound II has to be researched further in order to determine which compound is actually causing the enrichment of fluorine in the surface.

The possibility of generating highly-enriched fluoropolymer films bearing surface exposed sulfonyl fluoride groups was shown. This method allows the strategy of forming fluoropolymer overlayer coatings using only little amounts of the expensive fluorinated epoxide monomer in conventional commercial aliphatic polymer resins.

Repetition of trials employing compounds I and II

Compound I showed inconsistent results that could not be explained. The experiments should be repeated to get consistent data. Trials for compound II were only run once and should also be repeated to test the repeatability of the result. In general, the experiments should be run not once but several times (the proper sample size would have to be determined) to obtain results that are statistically valid.

Increase % wt of compound II

The trials with compound II, using the surfactant to prevent phase separation, have been conducted with relatively low concentrations of the fluoroepoxide. Experiments should be performed that involve an increase in the amount of compound II . The use of surfactant was promising and might allow for much higher concentrations of this compound in the polymerization.

Chainlength study

A study could be run that involves epoxides of different chain lengths. A relationship between the percentage of fluorine enrichment in the film versus the length of a perfluorinated carbon chain could be established. It is known that carbon chains of C6 and longer are very likely to migrate to the surface. Increasing this length even more will yield valuable insight in the characteristics of monomer-migration.

Study of group sizes in fluoroepoxides

Compound III is the epoxide that was polymerized with the greatest success. It showed the most fluorine surface enrichment and was repeatable. A study that experiments with different group sizes could be conducted. Bulkier groups will most likely show more surface enrichment and might be easy and successful to polymerize.

Duration of surface properties

The duration of the surface properties of films enriched with perfluorinated epoxides in the surface region should be studied. The surface of a polymer film is not stable over time, it is dependent on properties of the environment (e.g., temperature, relative humidity). A study should determine for how long the films synthesized in this study are stable in their surface properties.

References

1. Shag Yen Lee and Caroll H Clatterbuck; Sampe Q, (1991), 22 (3) 52-7

2. Shag Yen Lee; US Patent US 87-108238

3. T. E. Twardowski and P.H. Geil; J. Appl. Polym. Sci, (1991) 42(6), 1721-6

4. Liliana Klinger; US Patent US 88-273444

5. Motonobu Kubo and Yoshiki Shimizu and Masato Kashiwagi and Tsutomu Kobayashi and Kozaburo Nakamura and Noria Murata; Japanese Patent, JP 88-99800

6. Sheng Yen Lee; Sampe Q, (1988), 19 (3), 44-8

7. Yutaka Yamada and Takao Doi and Shigeyuki Ozawa; Japanese Patent, JP 87-110794

8. J. R. Griffith and J. G. O'Rear; Polym. Sci. Technol. (Ptenum), (1987), 35 (Adv. Biomed. Polym.) 63-7

9. Sheng Yen Lee and James R. Griffith; Ind. Eng. Chem. Prod. Res. Dev., (1986), 25 (4), 572 -7

10. United States Dept. of the Army; US Patent, 83-508957

11. James R. Griffith; Amer. Paint J., (1972), 57 (1), 51-2

12. J. G. O'Rear and J.R. Griffith; Am. Chem. Soc., Div. Org. Coat. Plast. Chem, Pap. (1973), 33 (1)

13. Henry Lee and Kris Neville; Handbook of Epoxy Resins; McGraw-Hill Book Company, copyright 1967

14. Arnost Reiser; The science and technology of resists, John Wiley & Sons, A Wiley Interscience Publication, 1989, New York

15. J. V. Crivello; UV curing: Science and Technology (S. P. Pappas Ed), pp 24-75, Technology Marketing Corp; Norwalk, CT, 1980

16. R W. Lenz; Organic Chemistry of Synthetic High Polymers, p. 247, Interscience, New York 1967

17. F. S. Dainton and J. J. Ivin; Q. Rev. Chem. Soc, (1958), 12, 61

18. E. Fischer; US Patent 3,236,784 (1966)

19. S. I. Schlesinger; Photogr. Sci. Eng., (1974), 18, 387

20. J. V. Crivello and J. H. W. Lam; J. Polym. Sci, Polym. Symp., (1976), 56, 383

21. J. V. Crivello and J. H. W. Lam; J. Polym. Sci, Poly. Chem., (1979), 17, 977

22. H. M. Wagner and M. D. Purbrick; J. Photogr. Sci, (1981), 29, 230

23. J. V. Crivello and J. H. W. Lam; J. Polym. Sci; Polym. Chem. Ed., (1979) 17, 2877, (1980), 18, 1021

24. J. V. Crivello and J. H. W. Lam; Macromolecules, (1981), 14, 1141

25. K. Mayer and H. Zweifel; J. Imaging Sci, (1986) 30, 174

26. K. Mayer and H. Zweifel; SME Tech. Pap; RadCure p. 417 (1985)

27. Harry R. Allcock and Frederick W. Lampe; Contemporary Polymer Chemistry, 2nd Ed., Prentice Hall, New York 1990

28. A. U. Schnurer and N. R. Holcomb and G. L. Gard and D. G. Castner and D. W. Grainger; accepted Feb. 1996 by Chemistry of Materials

29. Application note from Surface Science Instruments, Mountain View, CA 1987

30. J. H. Scofield; J. Electron. Spectroscopy, Related Phenom., (1976), 8, 129

31. M. P. Seah, W. A. Dench; Surface Interface Anal., (1979), 1, 2

32. D. W. Grainger and T. Okano and S. W. Kim and D. G. Castner and B. D. Ratner and D. Briggs and Y. K. Sung; J. Biomed. Mat. Res., (1990), 24, 547

33. P.Tarrant and C.G.Allison and K.P. Barthold and E.C. Stump; Fluorine Chem.Rev., (1971), 5, 77

34. Steve Ullrich; M. S. Thesis, Portland State University, (1994)

35. N. N. Hamel and G. A. Russell and G. L. Gard; J. Fluorine Chem. (1994), 66, 105

36. F. Sun and D. G. Castner and G. Mao and W. Wang and P. McKeown and D. W. Grainger; Polym. Prep. (1994), 35(1), 774-5

37. Li-Fo Chen and Javid Mohtasham and Gary L. Gard; J. Fluorine Chem, (1990), 48, 107-122

38. S. C Yoon and B. D. Ratner; Macromolecules, (1986), 19, 1068

39. L. Lavielle and J. Schultz; J. Colloid Interface Sci., (1985), 106, 438

40. L. Lavielle and J. Schultz; J. Colloid Interface Sci., (1985), 106, 446

41. J. R. Rassmussen and D. E. Bergbreiter and G. M. Whitesides; J. Am. Chem. Soc., (1977), 99, 4746

42. E. Ruckenstein and S. V. Gourisankar; J. Colloid Interface Sci, (1985), 107, 488

43. H. Yasuda and E. J. Charlson and E. M. Charlson and T. Yasuda and M. Miyama and T. Okuno; Langmuir, (1991), 7, 2394

44. B. D. Ratner and P. K. Weathersby and A. S. Hoffman and M. A. Kelly and L. H. Scharpen; J. App. Poly. Sci, (1978), 22, 643

45. K. Takamori and N.-J. Jo and A. Takahara and T. Kajiyama; Rep. Prog. Polym. Phys. Jpn. (1987), 30, 57

46. A. Takahara and N.- J. Jo and K. Takamori and T. Kajiyama; "Progress in Biomedical Polymers", 1990 Plenum, New York, p. 217

47. K. G. Tingey and J. D. Andrade and R. J. Zdrahala and K. K. Chittur and R. M. Gendreau; " Surface Characterization of Biomaterials" (B. D. Ratner, Ed.) 1988, Elsevier, Amsterdam, p. 255

48. Z. Deng and H. P. Schreiber; J. Adhesion (1991), 36, 71

49. F. J. Holly and M. F. Refojo; J. Biomed. Mater. Res., (1975), 9, 315

50. F. J. Holly and M. F. Refojo; ACS Symp. Series, (1976), 31, 252

51. J. D. Andrade and R. N. King and D. E. Gregonis; ACS Symp. Series, (1976), 31, 206

52. S. H. Lee and E. Ruckenstein; J. Colloid Interface Sci. (1987), 120, 529

53. M. M. Dorff and E. Lindner; Macromolecules, (1989), 22, 2951

54. J. Hopken and S. Sheiko and J. Czech and M. Moeller; Polym. Prepr. (Am. Chem. Soc., Div Polym. Chem.), (1992), 937

55. G. A. Olah and P. S. Iyer and P. Sura; Synthesis, (1986), 513

56. N. Hamel and G. L. Gard; J. Fluor. Chem., (1994), 68, 253

57. J. M. Canich and M. M. Ludvig and G. L. Gard and J. M. Shreeve; Inorg. Chem., (1984), 23, 4403

58. R. J. Terjeson and J. Mohtasham and R. M. Sheets and G. L. Gard; J. Fluorine Chem., (1988), 38, 3

59. M. J. Browden; Macromolecules (F. A. Bovey and F. H. Winslow, Eds), Chap. 2, Academic, New York, 1979

60. N. N. Hamel; Ph. D. Thesis, Portland State University, (1995)

61. Li-Fo Chen and Javid Mohtasham and Gary L. Gard; Journal of Fluorine Chemistry, (1990), 48, 107 -122

Figure 14 IR-Spectra of sample A and B

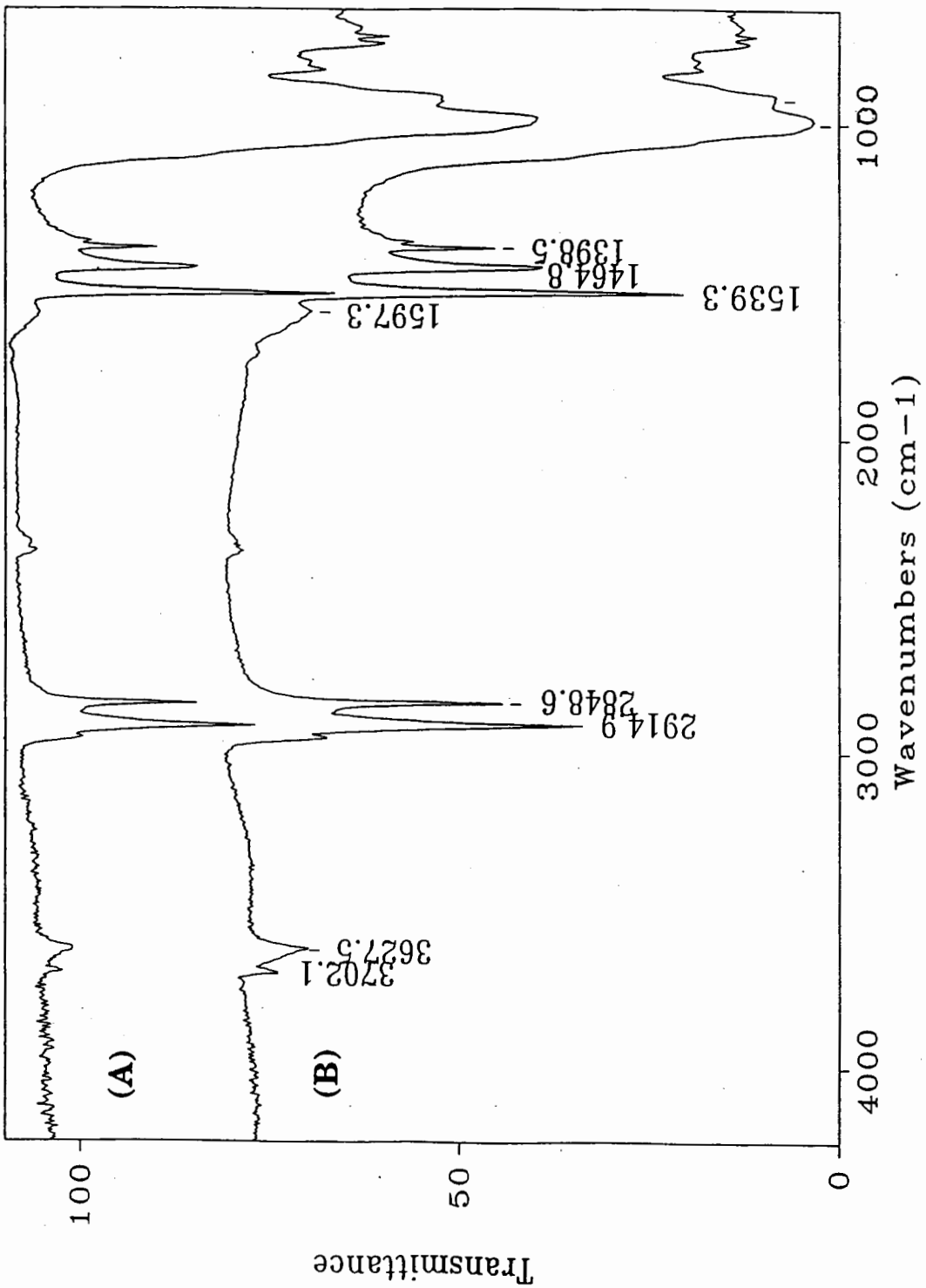

Figure 15 IR-Spectra of sample C and D

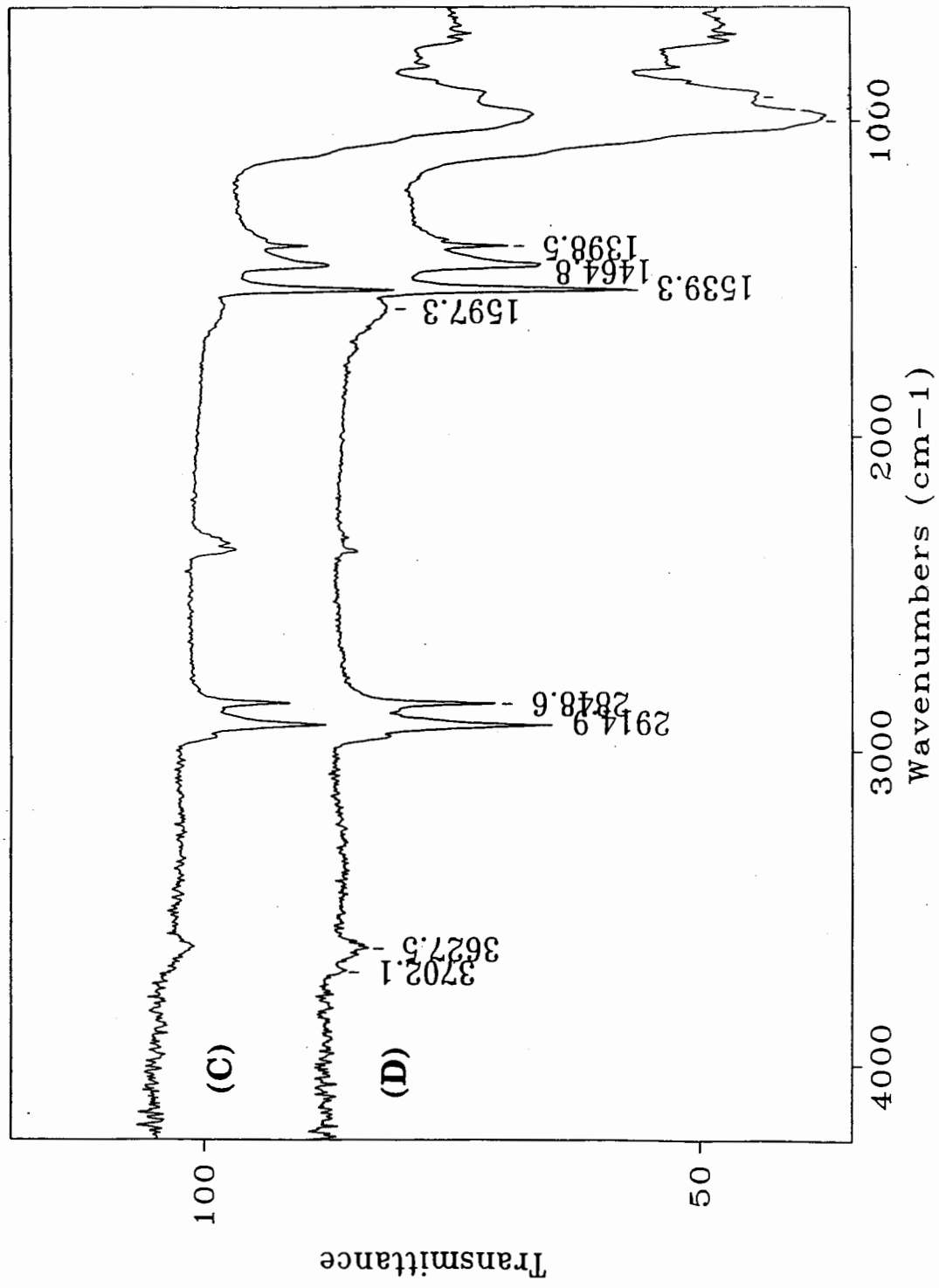

Figure 16 SSIMS Spectra of compound I